JOURNAL OF GEOPHYSICAL RESEARCH, VOL. 86, NO. B11, PAGES 10569-10590, NOVEMBER 10, 1981

HYBRID GRANODIORITES INTRUDING THE ACCRETIONARY PRISM, KODIAK, SHUMAGIN, AND SANAK ISLANDS, SOUTHWEST ALASKA

Malcolm Hill[1]

Earth Sciences Board, University of California, Santa Cruz, California 95064

Julie Morris

Center for Geoalchemy, Department of Earth and Planetary Sciences, Massachusetts Institute of Technology, Boston, Massachusetts, 02139

Joseph Whelan

Isotope Branch, U.S. Geological Survey, Denver, Colorado 80225

Abstract. A narrow belt of tonalite-granodiorite-granite plutons and batholiths intruded the accretionary prism in southwestern Alaska about 60 m.y. ago, simultaneously with plutonism over 100 km north along the main arc axis. The presence of metasedimentary xenoliths, kyanite, and garnet within the intrusions exposed on the Kodiak, Shumagin and Sanak islands establishes the presence of a crustal component. Extremely high values of $\delta^{18}O$, from +10.9 to +13.2 o/oo, require a crustal origin for much of the oxygen in the intrusions. Open-system alteration has disrupted whole-rock Rb-Sr systematics in some samples from the Sanak pluton and Shumagin batholith. Mineral isochrons using unaltered minerals yield an age of 58.7 ± 1.2 m.y. and $^{87}Sr/^{86}Sr_i$ = 0.70534 ± 10 for the Shumagin batholith, and ages of 62.7 ± 1.2 m.y. and $^{87}Sr/^{86}Sr_i$ = 0.70523 ± 14 for the Sanak pluton. Comparison of the isotopic data for the intrusions with those of sedimentary rocks in the Kodiak and Shumagin formations requires that a low-$\delta^{18}O$, low-$^{87}Sr/^{86}Sr$ component be present as well. Mixing models combining $^{87}Sr/^{87}Sr$ and Sr contents of various kinds of mafic magmas with partial melts of metasedimentary wall rocks suggest that three types of mafic magmas can satisfactorily duplicate the oxygen isotope signature of the intrusions: (1) a mid ocean ridge (MORB)-like magma, (2) a magma derived by partial fusion of altered MORB, or (3) an arc basalt. The MORB model predicts abundances of Rb, Sr, Ba, and rare earth elements which are similar to those in the intrusions, while the altered MORB model does not. The arc magma model provides a better trace element match than the remelted MORB model, but is not as successful as the MORB model. These intrusions were preceded by a pulse of mafic to intermediate volcanism near or within the accretionary prism, recorded in the Paleocene Ghost Rocks Formation. This volcanism is probably the heat and mass source of the mafic component within the intrusions, and may be related to activity of the Kula-Farallon ridge approximately 60 m.y. ago.

Introduction

A narrow arcuate belt of plutons intruded Upper Cretaceous sedimentary rocks along the continental margin of southwest Alaska 60 m.y. ago. The intrusions range from biotite tonalite to granite and vary in size from the small pluton on Sanak Island to batholiths on Kodiak and the Shumagin islands (Figure 1). Here we attempt to determine the source rocks which melted to form these intrusions. In order to do this, it is necessary to distinguish between characteristics imposed by the source material(s) and those caused by other processes such as fractional crystallization, hydrothermal exchange with wall rocks, and postcrystallization alteration or metamorphism.

To separate these effects we have determined major and trace element concentrations, Sr and O isotopic compositions for whole rocks, and Sr isotopic compositions for mineral separates from selected samples. Trace elements can be used as sensitive indicators of fractionation processes, postsolidification alteration, and, if these effects can be thoroughly evaluated, source characteristics. Sr isotope ratios do not change during fractional crystallization, and so give information on the nature of the source(s) assuming that alteration effects can be 'seen through', if present. In this study, some alteration has occurred, and we use the mineral isochrons to help evaluate its extent. Oxygen isotopes are not appreciably fractionated during fractional crystallization (less than about 2o/oo [Matsuhisa et al., 1973]). At the high temperatures required for partial melting, the $\delta^{18}O$ of the magma will be similar to that of its source rocks. This signature can be affected by post-intrusion hydrothermal exchange, but intrusions which have suffered extensive exchange with their wall rocks typically display concentric zonation of $\delta^{18}O$ [Taylor, 1978]; samples chosen for geographic coverage across an intrusion can help evaluate this possibility.

Field Relations and Age

Volcanic and plutonic rocks have been generated at intervals throughout the Mesozoic and Cenozoic in southwest Alaska [Burk, 1965; Reed and Lanphere, 1969, 1973; Hudson, 1979], presumably in relation to the subduction of oceanic

[1]Now at Earth Sciences Department, 14-HO, Northeastern University, Boston, Massachusetts 02115.

Paper number 1B0904.
0148-0227/81/001B-0904$01.00

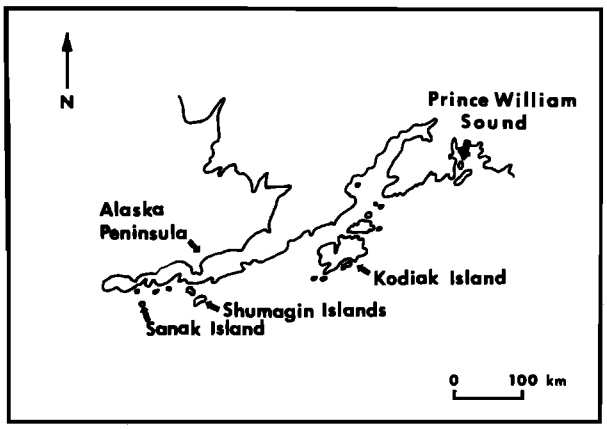

Fig. 1. General location map of southwestern Alaska showing the locations of the Kodiak and Shumagin batholiths and the Sanak pluton.

lithosphere. Most of this activity occurred along and north of the present-day belt extending from Sanak Island northeast through the Shumagin and Kodiak islands toward Prince William Sound (Figure 1), and lie more than 100 km nearer the axis of the presumed early Tertiary subduction zone than coeval intrusions along the magmatic arc axis. Our samples, from the southwestern part of this belt, were collected by J. C. Moore during mapping of the Sanak and Shumagin islands, and by the senior author along Three Saints Bay on Kodiak Island (Figure 2). Hudson et al. [1979] describe plutons from the northeastern part of this belt, near Prince William Sound.

The Kodiak, Shumagin, and Sanak islands consist largely of a series of probably accreted terranes ranging from Early Jurassic to Eocene in age [Burk, 1965; Connelly, 1978; J. C. Moore, 1973a, b, 1974a, b; G. W. Moore, 1967, 1969; Fisher and Holmes, 1980]. Structural deformation is complex in all accreted units, yielding broken formations and tectonic melange. Formations generally are fault-bounded. The trend of regional tectonic structures, including major faults and foliation within the deformed units, is parallel to the present-day continental margin.

The three intrusions we have studied intrude Upper Cretaceous (Maestrichtian, 73-66 m.y. [Lanphere and Jones, 1978]) graywacke and argillite of the Kodiak Formation on Kodiak Island and the correlative Shumagin Formation on the Shumagin and Sanak islands [Connelly, 1978; Nilsen and Moore, 1979; J. C. Moore, 1974a, b]. Small satellite plutons, probably related to the Kodiak batholith, intrude the graywacke-, argillite-, and greenstone-bearing Ghost Rocks Formation of Kodiak Island [Connelly, 1978; G. W. Moore, 1967, 1969; Reid and Gill, 1980], which contains fossils tentatively dated as Paleocene [Nilsen and Moore, 1979] (approximately 65-45 m.y. [Hardenbol and Berggren, 1978]). K-Ar biotite and muscovite ages for the Kodiak, Shumagin, and Sanak intrusions are generally concordant in samples where both have been analyzed, and cluster around 60 m.y. [Burk, 1965; Kienle and Turner, 1976; Turner et al., 1973]. These ages suggest that the Ghost Rocks Formation was deposited in the earliest Paleocene, between 60 and 65 m.y. ago. This point becomes important when we consider the origin of the intrusions.

The contacts of the Tertiary intrusions on the Kodiak, Shumagin and Sanak islands are locally

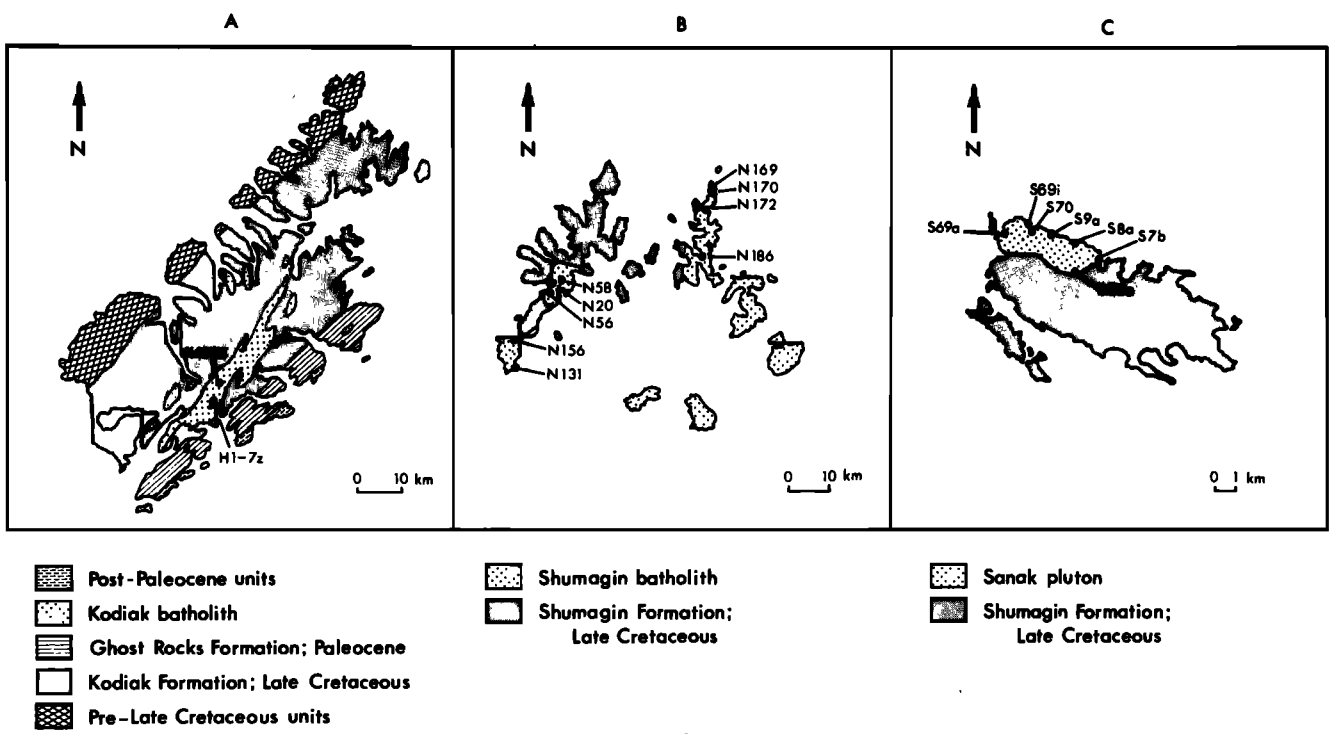

Fig. 2. Generalized geologic maps of the (a) Kodiak, (b) Shumagin, and (c) Sanak islands with sample locations for intrusive rocks. Geology is after G. W. Moore [1967], Connelly, [1978], Connelly and Moore [1977], Grantz [1963], and J. C. Moore [1974a, b].

discordant with the trends of fold axes in the country rocks [J. C. Moore, 1974a, b]. However, on a regional scale both the Kodiak batholith and its smaller satellite plutons are elongate parallel to the regional tectonic grain, suggesting structural control of the shapes of the intrusions. No strong foliation or protoclastic fabric was observed in any of the intrusions. The Kodiak and Shumagin formations have been metamorphosed to biotite- and andalusite-bearing hornfels within about 500 m of the contacts (T. Byrne, personal communication, 1980). Regional metamorphism away from the intrusions has not been extensively studied; the Shumagin Formation contains laumontite and prehnite [J. C. Moore, 1973b and personal communication, 1980], and Connelly [1978] described prehnite and pumpellyite from the Ghost Rocks Formation.

Petrography

The intrusions are composed of biotite tonalite, biotite granodiorite, and biotite granite (Table 1) (International Union of Geological Sciences (IUGS) classification [Streckeisen, 1973]). The samples in the IUGS granite field would fall in the quartz monzonite field of Bateman et al. [1963]. Biotite is the sole ferromagnesian silicate. Muscovite, where present, generally replaces biotite, plagioclase, or orthoclase. Rarely, muscovite forms euhedral, possibly primary crystals. In all sections, FeTi oxides, apatite, and zircon occur as inclusions in most minerals. Most samples have been sericitized, and locally biotite has been chloritized. The freshest samples were chosen for detailed geochemical studies, but none are completely free of these effects.

Xenocrysts and partially digested inclusions of probably metasedimentary origin are common in all three intrusions. The inclusions range in size from less than 1 cm to more than 6 cm in diameter. They contain the same minerals present as phenocrysts in the intrusions: biotite, plagioclase, quartz, perthitic orthoclase, and some muscovite. In addition, some contain garnet and kyanite. Kyanite xenocrysts are surrounded by reaction rims of a fine-grained, high-relief mineral which may be sillimanite; kyanite should not be stable at magmatic temperatures. The garnets have no reaction rims but are anhedral. We consider the clots and kyanite and garnet xenocrysts to be relicts of partially digested amphibolite-grade metamorphic rocks, which could represent either residual material not melted in the source region or accidental contaminants derived from the wall rocks. In either case, the xenocrysts and inclusions establish the presence of a metasedimentary component in the intrusions.

Geochemistry

Samples from the Kodiak and Shumagin batholiths, the Sanak pluton, graywacke and argillite from the Kodiak and Shumagin formations, and greenstones from the Ghost Rocks Formation have been analyzed for major and trace elements, and selected samples for Sr and O isotopes, by methods described below. Additional major and trace element analyses for plutonic, volcanic and sedimentary rocks from this area are given in the works by Hill [1979] and Reid and Gill [1980].

Analytical methods. Major and minor elements were analyzed by X ray fluorescence (XRF) on a Phillips PW1410 spectrometer at the University of California at Santa Cruz, using glass pellets prepared after Norrish and Hutton [1969] and Harvey et al. [1973]. Pressed powder pellets were used for XRF determination of Na and trace elements (Zr, Y, and some Ba analyses in Table 2). Additional trace elements (Cs, Ba, rare earth elements (REE), Ta, Hf, Sc, Co) were obtained by instrumental neutron activation at the NASA-Johnson Space Center in Houston (samples S70, N20, H1-7z, K4033, U13a, M5c, and 15-2e), the U.S. Geolological Survey in Denver (S7b, S8a, S69a, S72d, S89d, and S233b), and at the Massachusetts Institute of Technology (MIT) in Cambridge (N131, N170, and N186). Methods used are similar to those described by Jacobs et al. [1977].

Oxygen isotopes were determined at the U.S. Geological Survey in Denver following standard techniques [Clayton and Mayeda, 1963]. Using a CO2-H2O fractionation factor of 1.0412, 14 analyses of NBS-28 [Friedman and Gleason, 1973] during the study gave a mean value of 9.97 ± 0.11 o/oo (1σ).

Rb and Sr contents and Sr isotope ratios were analyzed at the Department of Earth and Planetary Sciences at MIT on a 9", 60° spectrometer using techniques given by Hart and Brooks [1977]. A Rb decay constant of 1.42×10^{-11} yr^{-1} [Steiger and Jaeger, 1977] was used for all calculations. All $^{87}Sr/^{86}Sr$ ratios are normalized to $^{86}Sr/^{88}Sr = 0.1194$ and are reported relative to Eimer and Amend SrCO3 = 0.70800. Reported uncertainties are 2σ of the mean.

Major and trace elements. SiO2 varies from 64.5 to 72.7% in the Sanak pluton, from 61.3 to 75.9% in the Shumaggin batholith, and three samples from the Kodiak batholith range from 63.8 to 68.6% (Table 2). On a normative Q-Ab-Or diagram, rocks from the three intrusions occupy different but partially overlapping fields near the minimum melting compositions for $P_{H2O} < 4$ kbar in the granite system [Tuttle and Bowen, 1958; Luth et al., 1964]. All samples are peraluminous with normative corundum from 0.4 to 4.4%. Na2O/K2O ratios are close to 1, and K/Rb ratios are between 249 and 273. Compositions vary more or less regularly within each intrusion and between different intrusions. For example, in Figure 3 note that the Kodiak batholith has the least K2O and the Sanak pluton the most K2O at a given SiO2 content, with Shumagin samples falling between the two.

All of these granitic rocks are light rare earth element (LREE) enriched (Figure 4). Although the magnitude of the europium anomaly increases smoothly with increasing SiO2, total rare earths increase, then decrease with increasing SiO2 for the Sanak and Shumagin intrusions (too few data are available for the Kodiak batholith to establish any trends). The REE contents of the sedimentary rocks of the Kodiak and Shumagin formations are also shown in Figure 4, with the Haskin et al. [1966] average of 40 North American shales for comparison. There is no systematic difference in REE contents between the graywacke and argillite samples, or between the sedimentary rocks from different islands.

Oxygen isotopes. Oxygen isotope data for the

TABLE 1. Sample Locations and Petrographic Descriptions of Analyzed Plutonic Samples

Sample	N. Latitude	W. Longitude	Description
		Sanak pluton	
S8a	54°28'28"	162°43'48"	Biotite granodiorite; 0.271 qtz + 0.394 plg. + 0.079 ksp + 0.231 bio + 0.01 ox + tr. ap + tr. zir + tr. ky + tr. gar
S9a	54°28'48"	162°45'07"	Biotite granodiorite; 0.301 qtz + 0.346 plg + 0.059 ksp + 0.213 bio + 0.007 ox + 0.003 ap + tr. zir + 0.004 mus + tr. ky
S69i	54°29'12"	162°46'52"	Biotite granodiorite; 0.242 qtz + 0.408 plg + 0.080 ksp + 0.246 bio + 0.002 ox + tr. ap + tr. zir + tr. gar + tr. mus
S70	54°29'09"	162°46'47"	Biotite granodiorite; 0.260 qtz + 0.44 plg + 0.07 ksp + 0.21 bio + 0.001 ox + 0.02 mus + tr. ap + tr. zir
S20a	54°27'08"	162°43'00"	Biotite granodiorite; 0.33 qtz + 0.38 plg + 0.07 ksp + 0.19 bio + 0.01 ox + 0.002 ap + 0.002 zir + 0.004 mus
S69a	54°28'46"	162°49'00"	Biotite granite; 0.29 qtz + 0.33 plg + 0.20 ksp + 0.16 bio + 0.003 ox + 0.002 ap + 0.002 zir + 0.01 mus
S7b	54°27'43"	162°41'38"	Biotite granite; 0.32 qtz + 0.32 plg + 0.29 ksp + 0.07 bio + 0.002 ox + tr. ap + tr. zir
S7a	54°27'43"	162°41'38"	Biotite granodiorite; 0.227 qtz + 0.445 plg + 0.183 ksp + 0.108 bio + 0.007 ox + 0.002 ap + 0.001 zir + tr. mus
		Shumagin batholith	
N131	54°52'48"	160°11'43"	Biotite tonalite; qtz + plg + bio + ox + tr. ap + tr. zir
N58	55°03'54"	160°02'38"	Biotite granodiorite; 0.196 qtz + 0.564 plg + 0.138 ksp + 0.080 bio + 0.004 ox + tr. ap + tr. zir
N186	55°06'12"	159°33'21"	Biotite granodiorite; 0.282 qtz + 0.521 plg + 0.062 ksp + 0.115 bio + 0.004 ox + 0.004 ap + 0.001 zir + 0.011 chl
N172	55°11'28"	159°32'17"	Biotite granodiorite; 0.272 qtz + 0.470 plg + 0.153 ksp + 0.101 bio + 0.001 ox + tr. ap + tr. zir
N20	55°02'40"	160°05'21"	Biotite granite; 0.436 qtz + 0.308 plg + 0.180 ksp + 0.070 bio + 0.002 ox + tr. ap + tr. zir + tr. chl + tr. mus
N56	55°02'04"	160°05'40"	Biotite granite; 0.221 qtz + 0.334 plg + 0.398 ksp + 0.044 bio + tr. ox + 0.002 ap + tr. zir
N156	55°56'00"	160°11'53"	Biotite granodiorite; 0.216 qtz + 0.476 plg + 0.239 ksp + 0.069 bio + tr. ox + tr. ap + tr. zir + tr. chl
N169	55°14'27"	159°39'19"	Biotite granite; 0.362 qtz + 0.294 plg + 0.272 ksp + 0.072 bio + tr. ox + tr. ap + tr. zir + tr. mus + tr. chl
N170	55°14'38"	159°30'38"	Granophyric granite; qtz, ksp, and zoned plg in granophyric intergrowth; tr. bio, ox, ap, zir
		Kodiak batholith	
H1-7z	57°10'46"	153°30'44"	Biotite tonalite; 0.28 qtz + 0.45 plg + 0.04 ksp + 0.20 bio + 0.003 ox + 0.008 ap + tr. zir + tr. mus
K4033			Biotite granodiorite; 0.27 qtz + 0.40 plg + 0.17 ksp + 0.13 bio + 0.001 ox + 0.002 ap + 0.003 zir + 0.02 mus

Abbreviations: ap = apatite; bio = biotite; chl = chlorite; gar = garnet; ksp = k-feldspar; ky = kyanite; mus = muscovite; ox = Fe-Ti oxide; plg = plagioclase; qtz = quartz; tr. = trace; zir = zircon.

Table 2a. Major Element Analyses of Sanak Pluton and Kodiak Batholith, Alaska

	Sanak Pluton								Kodiak Batholith	
	S8a	S9a	S69i	S70	S20a	S7a	S69a	S7b	H1-7z	K4033
SiO_2	64.54	64.97	65.22	65.45	66.01	66.18	68.90	72.74	65.76	68.56
TiO_2	0.90	0.82	0.79	0.82	0.79	0.72	0.54	0.20	0.63	0.52
Al_2O_3	15.71	15.83	15.57	15.41	15.64	15.47	14.85	13.66	15.91	15.80
Fe_2O_3*	6.55	6.24	5.87	5.89	5.87	5.37	4.13	2.26	4.22	2.82
MnO	0.10	0.09	0.09	0.08	0.10	0.09	0.07	0.05	0.08	0.07
MgO	1.96	1.77	1.66	1.74	1.63	1.43	0.93	0.29	2.29	1.19
CaO	2.37	2.10	2.26	2.30	2.10	2.09	1.63	0.85	3.40	2.63
Na_2O	2.82	2.86	2.81	3.20	2.58	2.74	3.18	4.16	2.49	2.99
K_2O	3.06	3.28	3.19	3.24	3.54	3.82	4.18	4.64	2.49	2.91
P_2O_5	0.26	0.23	0.23	0.24	0.22	0.21	0.20	0.18	0.20	0.20
LOI	1.19	1.28	1.75	1.36	1.09	1.23	1.18	1.24	1.03	0.83
Total	99.46	99.47	99.44	100.13	99.57	99.35	99.79	100.27	98.50	98.52

*Total iron as Fe_2O_3.
LOI = Loss on Ignition. All other data by XRF.

intrusive and sedimentary rocks are presented in Table 3 and summarized in Figure 5. In the intrusive rocks, $\delta^{18}O$ ranges from +10.9 to +13.2 o/oo. These are extremely high values for igneous rocks and require a crustal source for much of the oxygen in the intrusions [Taylor, 1978]. Although the data scatter, samples with greater SiO2 and lower TiO2 and total Fe tend to have slightly higher positive $\delta^{18}O$ values, perhaps due to fractional crystallization. Except for one sample from the very edge of the Sanak pluton (S7b), there is no systematic zonation of $\delta^{18}O$ within the intrusions. We conclude that the high positive $\delta^{18}O$ of the intrusive rocks is a primary feature of the magma and is not the result of postintrusion, hydrothermal exchange with the sedimentary wall rocks.

Graywackes from the Upper Cretaceous wall rocks partly overlap the $\delta^{18}O$ range for the intrusions, but extend to higher values. Argillites have even heavier oxygen, as expected from their higher clay mineral contents [Savin and Epstein, 1970].

Strontium isotopes. Rb, Sr, and Sr isotopic compositions for 21 granitic whole rocks, four sets of mineral separates, and 11 sedimentary rocks are presented in Table 3. The granitic samples were chosen to give geographic coverage of the intrusions and to cover the range of major and trace element variation.

The whole rock data for the intrusions are plotted in Figure 6. The Shumagin batholith samples scatter somewhat, defining an 'errorchron' with an apparent age of 59.8 m.y. and an initial $^{87}Sr/^{86}Sr$ of 0.70482. The Sanak pluton shows less scatter, but gives an 'age' of 49.5 m.y., substantially younger than the 60 m.y. K-Ar ages reported [Burk, 1965; J. C. Moore, 1974b]. The scatter of points about the best fit lines and the young age for the Sanak pluton suggest that closed system models cannot be applied to these intrusions. Alteration and (or) initial isotopic heterogeneity could explain this behavior.

In an attempt to explain the scatter of data and the young age for the Sanak pluton, we analy-

Table 2b. Major Element Analyses of Shumagin Batholith, and a Greenstone from the Ghost Rocks Formation, Alaska

	Shumagin Batholith									Greenstone, Ghost Rocks Formation
	N131	N58	N186	N172	N20	N56	N156	N169	N170	15-2e
SiO_2	61.32	67.78	68.03	69.60	73.24	73.32	74.54	74.79	75.94	52.14
TiO_2	1.07	0.42	0.63	0.50	0.24	0.24	0.18	0.21	0.08	0.91
Al_2O_3	16.81	15.53	15.36	14.79	13.87	13.72	13.49	13.34	12.87	15.41
Fe_2O_3*	7.15	3.00	4.38	3.72	2.24	2.27	2.15	1.84	1.42	7.74
MnO	0.11	0.06	0.07	0.06	0.04	0.04	0.05	0.04	0.04	0.12
MgO	2.73	1.37	1.46	1.07	0.45	0.41	0.16	0.38	0.02	7.42
CaO	3.94	2.84	2.69	2.39	1.27	1.13	1.16	0.73	0.51	7.08
Na_2O	2.86	4.03	3.54	3.53	4.13	4.27	4.13	3.95	3.84	4.10
K_2O	2.19	2.91	3.95	3.51	4.01	4.01	4.00	4.42	4.72	0.27
P_2O_5	0.24	0.10	0.13	0.12	0.08	0.08	0.08	0.09	0.07	0.14
LOI	0.91	1.67	1.08	0.85	0.94	1.04	0.63	0.97	0.73	3.92
Total	99.33	99.71	100.32	100.15	100.51	100.53	100.57	100.76	100.24	99.25

*See footnotes for Table 2a.

Table 2c. Major Element Analyses of Mesozoic Sedimentary Rocks, Kodiak, Shumagin and Sanak Islands, Alaska

	Kodiak Formation		Shumagin Formation (Shumagin Islands)						Shumagin Formation (Sanak Island)				
	Graywacke	Argillite	Graywacke				Argillite		Graywacke			Argillite	
	U13a	M5c	N16a	N18b	N62	N65	NY90	N42b	N135	S84f	S72d	S233b	S33e	S89d
SiO_2	71.62	61.30	65.08	61.09	70.05	63.86	66.77	59.37	58.55	61.50	61.39	63.93	60.79	58.88
TiO_2	0.63	0.84	0.60	0.69	0.53	0.71	0.68	0.76	0.81	0.72	0.79	0.67	0.82	0.81
Al_2O_3	11.72	15.94	14.87	15.65	12.78	15.99	14.34	17.87	23.19	17.22	15.47	13.38	16.58	16.60
Fe_2O_3*	3.95	6.83	5.69	5.78	4.47	5.35	4.40	7.49	5.44	5.76	6.20	5.66	6.75	6.92
MnO	0.05	0.10	0.11	0.12	0.06	0.10	0.10	0.10	0.11	0.12	0.15	0.12	0.10	0.10
MgO	1.54	2.32	1.87	2.66	1.59	2.20	1.57	3.09	2.13	1.99	1.89	2.09	2.62	2.57
CaO	1.35	1.02	2.69	3.61	1.34	2.81	2.17	1.09	0.40	2.00	1.93	2.83	1.63	1.34
Na_2O	3.01	1.19	2.84	3.24	2.47	3.46	4.20	0.76	1.51	4.29	4.39	3.10	1.79	2.07
K_2O	0.93	2.50	1.20	1.43	2.36	1.67	1.46	2.91	3.73	1.45	1.45	0.95	2.62	2.74
P_2O_5	0.13	0.23	0.14	0.23	0.15	0.19	0.19	0.18	0.15	0.17	0.17	0.14	0.22	0.22
LOI	3.21	5.53	3.21	3.11	2.65	3.22	2.13	4.52	4.23	3.20	2.77	5.32	5.05	5.31
Total	98.14	97.80	98.30	97.61	98.25	99.56	98.01	98.14	100.25	98.42	97.60	98.19	98.97	97.56

*See footnotes for Table 2a.

zed mineral separates from four whole rocks. The whole rocks were chosen to provide examples of samples which plot on the whole rock isochron (N20, S70) and ones which fall off the isochron (N131, S9a).

Compared with fresh plagioclase, sericitized plagioclase has greater Rb and Sr contents, as well as higher $^{87}Sr/^{86}Sr$ ratios. The Rb/Sr ratio of the altered plagioclase is higher in two out of three cases. These relationships can be seen in the mineral isochrons (Figure 7), which show that the samples differ greatly in degree of open-system behavior. N131 shows no alteration effects (there is no altered plagioclase), and the two minerals and the whole rock define a good isochron. N20 shows greater alteration, having sericitized plagioclase and cloudy K-feldspar; no three points lie on the same line for this sample. The initial $^{87}Sr/^{86}Sr$ ratio defined by N131 (0.70534 ± 10) is different at the 95% confidence level from that obtained from the whole rock errorchron (0.70482 ± 18). From the present data we cannot evaluate whether all of the Sr isotope heterogeneity for the Shumagin batholith reflects secondary alteration or whether some is due to initial heterogeneity inherited from the source(s). It is clear from sample N20 that secondary, open-system behavior is responsible for at least some of the variability. Nonetheless, the ages determined from the mineral isochrons (approximately 60 m.y.) are in good agreement with K-Ar results and with geologic relationships.

The situation for the Sanak samples is somewhat different, as the mineral isochrons give older ages than the whole rock isochrons. This would seem to indicate closed-system behavior for the minerals, but open-system relations for the whole rocks, exactly the opposite of the systematics usually described [Faure, 1977].

We have considered several possible explanations for these anomalous whole rock:mineral relationships. A real thermal event of 49 m.y. age is not a suitable explanation, as it would reset the mineral isochrons as well as those for the whole rocks. Alternatively, if the whole rock points defined a line of negative slope on a $(^{87}Sr/^{86}Sr)_o$ vs. Rb/Sr (pseudoisochron) diagram, the rotation of the isochrons through time would produce an apparent age for the whole rock isochron which is less than the real age. This suggests that the sources for the granitic rocks lay along a mixing line; however, this model runs into difficulties because of the implausibility of and end-member component which is mafic in character with Rb/Sr > 1.25 and $^{87}Sr/^{86}Sr$ < 0.7045.

A third model involves partial alteration of the whole rocks. This needs to be a systematic alteration or it would produce the random scatter about the isochron seen in the Shumagin case, rather than rotation of the whole rock isochron from a steeper to a shallower slope, corresponding to an apparent young age, as seen in Sanak. An alteration of this sort, affecting grain boundaries and some altered minerals, would not show up in a mineral isochron based on analysis of fresh minerals. Mechanisms for this include loss of common Sr recently or loss of radiogenic Sr through time.

These results suggest that alteration, primar-

Table 2d. Trace Element Analyses of Tertiary Intrusives, Kodiak, Shumagin, and Sanak Islands, Alaska

	Sanak Pluton				Shumagin Batholith				Kodiak Batholith	
	S8a	S70	S69a	S7b	N131	N186	N20	N170	H1-7z	K4033
Cs	5.5	6.8	6.5	2.8	4.0	6.2	7.9	9.0	6.8	2.9
Ba	898.	851.	898.	421.	917.	866.	—	603.	874.	721.
U	3.28	3.40	5.85	5.19	1.73	—	3.37	3.26	---	---
Th	6.84	11.2	8.18	5.55	5.0	11.6	8.7	6.7	7.3	7.8
Y	36.	35.	32.	17.	24.	46.	35.	28.	17.	24.
La	24.9	31.9	24.3	10.6	21.0	31.1	23.1	10.82	23.0	21.4
Ce	48.9	74.	48.4	22.44	48.	75.	52.1	28.9	48.5	45.5
Nd	26.0	—	26.0	13.8	23.	31.	—	14.	—	---
Sm	6.8	7.8	5.69	2.92	5.33	7.17	6.0	3.87	5.2	5.3
Eu	1.29	1.24	0.861	0.384	1.50	1.33	0.7	0.183	0.83	0.67
Gd	6.95	—	6.61	3.50	—	—	---	---	---	---
Tb	1.10	1.17	1.13	0.664	0.84	1.24	0.97	0.76	0.76	0.88
Tm	0.512	—	0.526	0.234	---	---	---	---	---	---
Yb	2.42	3.33	2.52	1.19	2.47	4.43	3.13	3.45	2.50	2.90
Lu	0.389	0.54	0.391	—	0.393	0.680	0.52	0.505	0.40	0.46
Ta	0.990	1.16	1.33	0.962	0.81	0.69	1.2	0.70	0.74	0.76
Zr	204.	210.	204.	110.	215.	232.	—	85.	---	---
Hf	5.47	7.1	6.02	3.08	6.7	7.0	5.1	2.8	5.7	4.2
Sc	16.0	15.3	10.5	6.98	21.71	13.59	11.0	4.27	14	9.5
Co	13.3	11.8	7.66	3.44	17.92	9.71	3.0	1.18	11.0	6.6
K/Rb	262.	269.	267.	360.	289.	373.	256.	231.	262.	249.
Rb/Sr	0.49	0.49	0.82	1.05	0.28	0.45	1.33	4.36	0.40	0.62
Ba/Rb	9.26	8.51	6.91	3.93	14.56	9.84	---	3.55	11.00	7.43
Ba/Sr	4.49	4.15	5.65	4.13	4.02	4.40	—	15.46	4.46	4.59
Th/U	2.09	3.29	1.40	0.94	2.89	—	2.58	2.06	---	---

Concentrations are in parts per million.
Ba (sample S70) and all Y and Zr data by XRF. Rb and Sr data from Table 3. All other trace elements by neutron activation.

Table 2e. Trace Element Analyses of Mesozoic Sedimentary Rocks and a Tertiary Greenstone, Kodiak and Sanak Islands, Alaska

	Shumagin Formation (Sanak Island)				Kodiak Formation		Ghost Rocks Formation
	Graywacke		Argillite		Graywacke	Argillite	Greenstone
	S72d	S233b	S33e	S89d	U13a	M5c	15-2e
Cs	0.32	2.6	5.3	5.2	1.7	6.3	0.22
Ba	968.	237.	923.	892.	352.	780.	---
U	1.52	1.35	2.46	2.54	---	---	---
Th	3.21	2.95	6.31	5.83	4.4	7.6	1.59
Y	24.	18.	25.	9.	20.	27.	5.
La	15.2	30.5	23.1	22.1	19.9	25.1	6.0
Ce	28.9	50.1	49.3	42.7	44.1	58.	15.7
Nd	23.7	25.0	26.0	18.1	---	---	---
Sm	3.36	3.78	5.22	4.63	4.01	5.5	2.8
Eu	1.15	1.00	1.25	1.30	0.98	1.38	0.77
Gd	4.30	3.76	4.46	4.21	---	---	---
Tb	0.76	0.52	0.75	0.78	0.53	0.88	0.70
Tm	0.450	0.337	0.446	0.484	---	---	---
Yb	2.07	1.32	1.90	2.47	1.85	2.88	2.34
Lu	0.281	0.154	0.304	0.258	0.312	0.48	0.36
Ta	1.05	1.13	0.846	0.734	0.55	0.9	0.25
Zr	---	---	---	---	---	---	86.
Hf	4.28	3.06	4.03	3.84	5.3	4.9	2.32
Sc	22.7	17.7	23.2	26.3	10.2	18.1	30.3
Co	32.3	29.6	24.2	27.6	14.2	18.3	28.5
K/Rb	502.	292.	275.	274.	266.	250.	320.
Rb/Sr	0.06	0.10	0.49	0.45	0.21	0.82	0.05
Ba/Rb	40.33	8.78	11.68	10.75	12.14	9.40	---
Ba/Sr	2.51	0.91	5.73	4.85	2.50	7.72	---
Th/U	2.11	2.19	2.57	2.30	---	---	---

Concentrations are in parts per million.
Ba (samples U13a, M5c) and all Y and Zr data by XRF. Rb and Sr data from Table 3. All other trace element data by neutron activation.

ily, rather than source heterogeneity, is responsible for the deviation from closed-system behavior. Heterogeneity, if present, is a minor effect. In later sections, we will model the Sanak pluton as an isotopically homogeneous body.

The data for the sedimentary rocks of the Kodiak and Shumagin formations are presented in Table 3. The graywacke Rb contents vary from 24 to 54 ppm, Sr from 136 to 492 ppm, and $^{87}Sr/^{86}Sr$ (calculated for 60 m.y.) from 0.70455 to 0.70498. The argillite Rb contents range from 86 to 125 ppm, Sr from 165 to 190 ppm, and $^{87}Sr/^{86}Sr$ (calculated for 60 m.y.) from 0.70607 to 0.70892. In addition to these differences controlled by lithology, there are also systematic differences in isotopic composition between samples from different islands. Ratios are highest for Kodiak sediments and become progressively lower westward along the arc.

The Causes of Major and Trace Element Variations Within the Intrusions

In this section, we examine the data in more detail in order to explain the geochemical variations within the intrusions. The intrusions display a number of common characteristics. Their trends on an Na-Ca-K diagram (Figure 8) are similar to many calc-alkaline intrusions. Projections of the trends of CaO vs. SiO2 and (Na2O + K2O) vs. SiO2 intersect in Peacock's [1931] calc-alkali (Sanak) and calcic (Shumagin, Kodiak) fields. Most elements display smooth trends on variation diagrams (Figure 3). K, Rb, Cs, Rb/Sr, and Ba/Sr are positively correlated with SiO2, while Fe, Mg, Sc, Co, (Cr), Eu, Eu/Eu* (europium anomaly), Sr, and (Ba) are negatively correlated with SiO2. The highly charged cations Zr, Hf, Ta, Th, U, and REE (except Eu) rise, then fall with increasing SiO2. Of the samples analyzed, the maximum abundances for these highly charged cations (except Ta) occur at 65.5% and 68.0% SiO2 for the Sanak pluton and the Shumagin batholith, respectively.

Several of the trends within the Sanak pluton and Shumagin batholith (increasing Rb, Sr, and Rb/Sr, and decreasing Eu/Eu* and ferromagnesian elements with increasing SiO2) are qualitatively consistent with fractional crystallization involving plagioclase + biotite ± Fe-Ti oxide. However, the behavior of the highly charged cations is not explained using major minerals alone, and no combinations of major and accessory minerals (apatite, zircon) have been found which can explain all of the trace element variations simultaneously. The negative correlation between REE and SiO2 in the Sanak and Shumagin intrusions is not uncommon in granitic rocks [Creasy et al., 1979; Crecraft et al., 1979; Frey and Chappell,

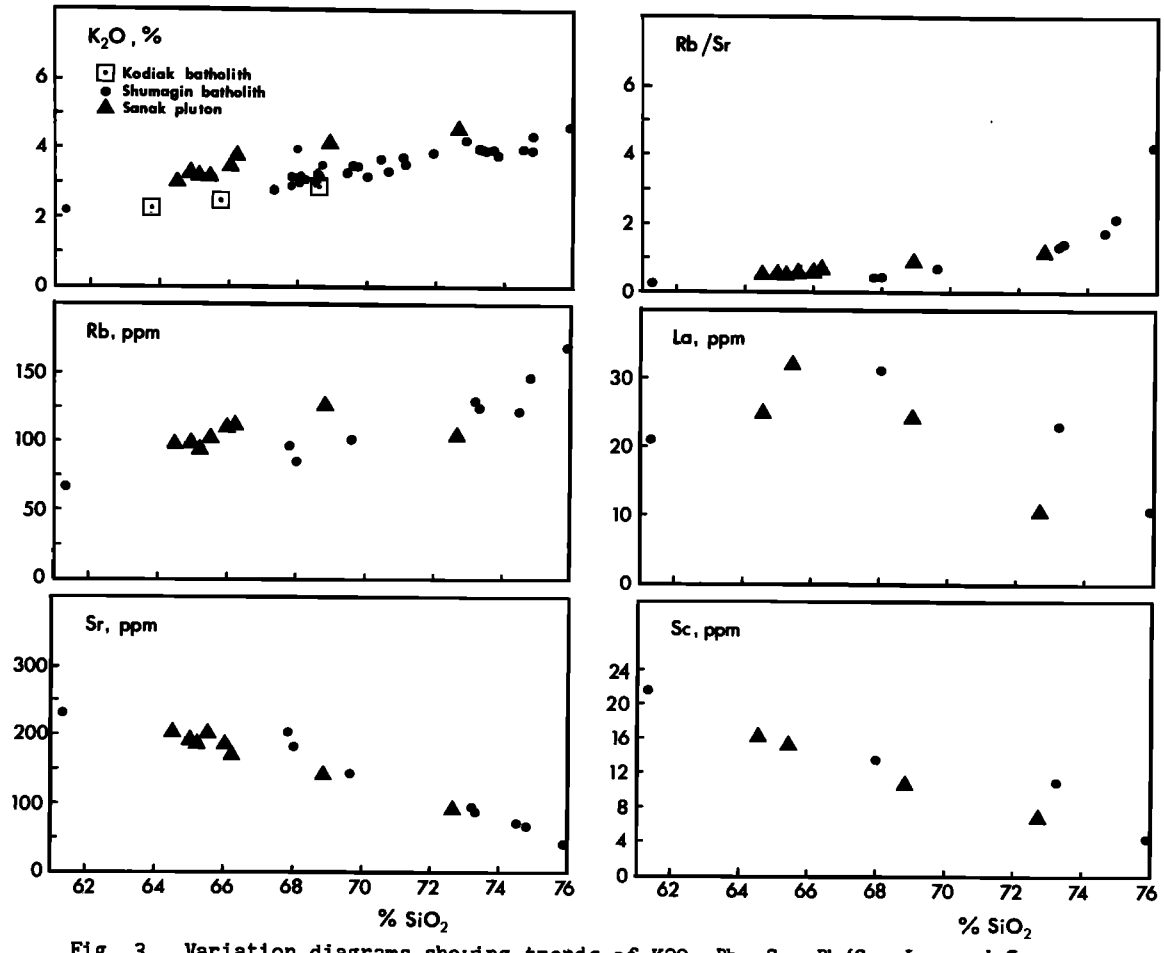

Fig. 3. Variation diagrams showing trends of K2O, Rb, Sr, Rb/Sr, La, and Sc vs. SiO2 for intrusive rocks from the Kodiak, Shumagin, and Sanak intrusions. K2O data are from Table 2 and Hill [1979]; remaining data are from Tables 2 and 3. Kodiak trace element data have been omitted for clarity.

1979; Luddington et al., 1979; Miller and Mittlefehldt, 1979], and no general solution has yet been provided to explain it.

We believe that crystal fractionation is responsible for generating most of the within-intrusion variations described above, modified by alteration as described in the previous section. Other processes which could conceibably generate these variations include (1) alteration alone; (2) mixing of two or more magmas without crystal fractionation; (3) local contamination with wall rocks; and (4) varying degrees of separation of melt from restite [White and Chappell, 1977].

Although the alkalies and (or) alkaline earths have been sufficiently mobile in some samples to obscure age information, the regular trends evident in Figure 3 argue against the hypothesis that alteration has had a dominant effect in establishing the observed element variations. Alteration would tend to increase the scatter of initially regular arrays of data, and it is improbable that alteration of unrelated samples would produce such regular variation patterns as those observed. Process 2 alone is unlikely because three different magmas would have to combine to explain the variations observed in the highly charged cations (La vs. SiO2, Figure 3). Since the Sanak pluton and Shumagin batholith show similar distributions of these elements, it would be necessary for the same kinds of magmas to combine in similar ways in two areas separated by more than 100 km.

While local wall rock contamination is probably responsible for the higher $\delta^{18}O$ of Sanak pluton sample S7b, process 3 fails as a general explanation for the regular geochemical trends because occasional assimilation of heterogeneous sedimentary rocks (Table 2) would produce random scatter on variation diagrams. This process might account for some of the fine-scale variations in Figure 3, but it cannot be responsible for the overall trends.

Finally, unless the accretionary prism was homogenized with respect to Sr isotopes prior to melting, process 4 cannot reconcile the variations observed in major and trace elements with the apparent Sr isotope homogeneity of the Sanak pluton. The most likely explanation for the chemical variations within the intrusions involves a melting event which produced an isotopically homogeneous magma, followed by fractional crystallization which changed the abundances of major and trace elements. More extensive isotopic anlysis of mineral separates from the Shumagin batholith is necessary to establish isotopic homogeneity for that body.

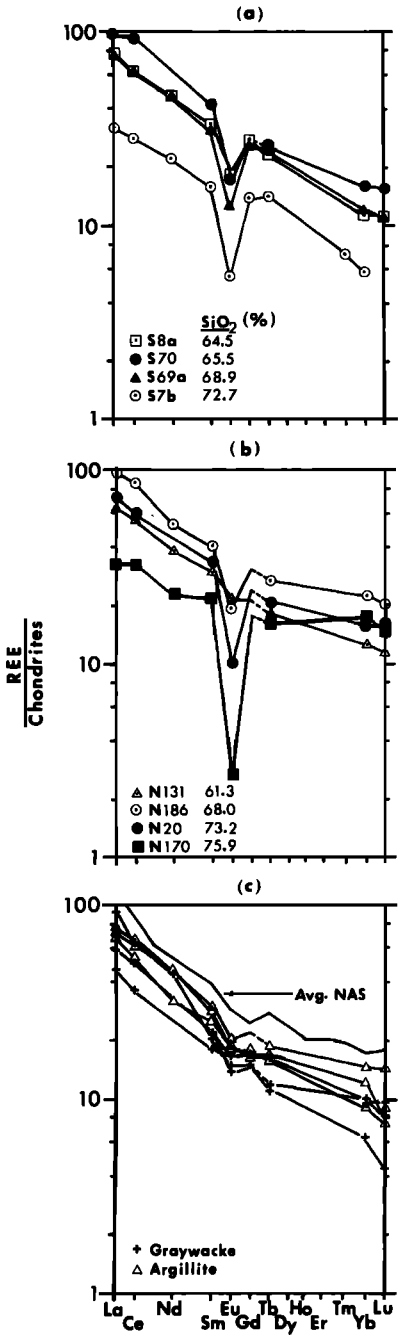

Fig. 4. Chondrite-normalized rare earth diagrams for (a) Sanak pluton, (b) Shumagin batholith, and (c) Upper Cretaceous graywacke and argillite of the Kodiak and Shumagin formations from Kodiak and Sanak islands. Avg. NAS is average of 40 North American shales from Haskin et al. [1966]. Kodiak batholith samples have been omitted for clarity.

Source Materials for the Intrusions

Hudson et al. [1979] proposed that the 50 m.y. old granodiorite intrusions near Prince William Sound, as well as those on the Kodiak, Shumagin, and Sanak islands, formed solely by melting within the accretionary prism. We disagree with this view, and argue below that an additional mafic or intermediate magma component, derived from beneath the accretionary prism, is also required. Our conclusions are based on a comparison of $\delta^{18}O$, Sr contents, and Sr isotopic compositions of the intrusions vs. potential sources in the prism. The models are discussed in a later section. In the following two sections we describe possible sources within and beneath the accretionary prism.

Sources within the accretionary prism. The oldest dated formation in the Kodiak-Shumagin-Sanak belt is the Upper Triassic greenstone- and graywacke-bearing Shuyak Formation [Connelly, 1978], exposed in the northern Kodiak Islands (Figure 2). One allocthonous block of Permian limestone occurs in the Uyak Complex [G. W. Moore, 1969], a tectonic melange which was emplaced after the mid-Early Cretaceous but before the Maestrichtian Kodiak Formation. The major point here is that ancient granitic or metamorphic crust is not likely to be present at depth: the nearest known Precambrian rocks are exposed well north of the Alaska Peninsula [Beikman, 1978]. The thin crust [Berg, 1973; Shor, 1962; Fisher and Holmes, 1980] further supports this conclusion.

Accretion in subduction zones apparently proceeds by the addition of younger units beneath older units [Karig and Sharman, 1975]. Assuming that this geometry applies to the Kodiak-Shumagin-Sanak area at 60 m.y. (and further, that the intrusions rose nearly vertically or at least did not form much nearer the Alaska Peninsula), it seems unlikely that the intrusions would have 'seen' any units within the accretionary prism older than the oldest ones they intrude at the surface - the Upper Cretaceous Kodiak and Shumagin formations. The only other unit which would have been in place 60 m.y. ago is the Ghost Rocks Formation, exposed on Kodiak Island. Accordingly, we have determined the geochemical characteristics of sediments from the Kodiak and Shumagin formations and a greenstone from the Ghost Rocks Formation (Tables 2 and 3).

It is important to estimate the relative proportions of greenstone, graywacke, and argillite in the accretionary prism. Unfortunately, no comprehensive studies of rock proportions exist for this area. Nilsen and Moore [1979] estimate sand:shale ratios of 1:1 to 1:5 for most of the Kodiak Formation, and ratios down to 1:30 for parts of it. The Ghost Rocks Formation may contain as much as 10% volcanic rocks, but very little greenstone or tuff occurs in the much more extensive Kodiak and Shumagin formations.

The Sr contents, $\delta^{18}O$, and $^{87}Sr/^{86}Sr$ ratios for Sanak Island graywacke and argillite used in Table 4 are taken from Table 3. We assume that the range of trace element and Sr and O isotopic variation we observe in the low-grade, metasedimentary rocks presently exposed at the surface would prevail through metamorphism to amphibolite facies at depth [Shaw, 1956; Sighinolfi and Gorgoni, 1978; Dostal and Capedri, 1978].

The concentrations of Sr and other trace elements in melts derived from metasediments depend on the values of D (distribution coefficient) for (bulk solid/liquid) chosen. Without experimental melting studies of graywacke and argillite which provide residual phase identities and proportions, comparable to those of Helz

Table 3. Rb and Sr Contents, and Sr and O Isotope Ratios For Tertiary Granitic and Mesozoic Sedimentary Rocks, Kodiak, Shumagin and Sanak Islands, Alaska

Sample		Rb ppm	Sr ppm	$^{87}Rb/^{86}Sr$	$^{87}Sr/^{86}Sr \pm 2\sigma$	$\delta^{18}O$ o/oo
Granitic Rocks						
Kodiak batholith						
H1-7z	w.r.	80.88	194.2	1.206	0.70651 ± 5	---
K4033	w.r.	99.7	157.0	1.839	0.70700 ± 7	---
Shumagin batholith						
N131	w.r.	65.5	231.0	0.821	0.70605 ± 6	11.4
	plag, fresh	3.95	459.2	0.025	0.70534 ± 4	---
	biotite	315.8	18.38	49.76	0.73914 ± 21	---
N58	w.r.	97.4	203.6	1.385	0.70544 ± 6	11.5
N186	w.r.	86.19	181.3	1.377	0.70610 ± 6	11.0, 10.8
N172	w.r.	103.1	145.1	2.058	0.70657 ± 4	11.3
N20	w.r.	129.5	95.7	3.919	0.70812 ± 9	12.0, 12.2
	plag, fresh	4.78	33.3	0.416	0.70443 ± 6	---
	plag, altered	108.9	166.9	1.890	0.70618 ± 6	---
	kspar	239.7	103.1	6.734	0.71012 ± 5	---
	biotite	626.3	12.69	142.9	0.82555 ± 36	---
N56	w.r.	126.0	88.0	4.147	0.70819 ± 8	12.9
N156	w.r.	123.3	70.9	5.040	0.70908 ± 5	11.5
N169	w.r.	148.2	68.2	6.291	0.71021 ± 5	12.1
N170	w.r.	170.0	40.2	12.25	0.71540 ± 4	12.5, 12.6
Sanak pluton						
S8a	w.r.	98.3	201.3	1.399	0.70662 ± 5	11.8, 12.0
S9a	w.r.	99.3	191.2	1.501	0.70684 ± 6	11.3
	plag, fresh	7.76	187.2	0.120	0.70559 ± 6	---
	plag, altered	13.08	442.	0.276	0.70567 ± 6	---
	kspar	78.6	339.8	0.670	0.70605 ± 6	---
	biotite	340.9	37.85	26.08	0.72521 ± 16	---
S69i	w.r.	97.3	187.1	1.506	0.70668 ± 7	11.2
S70	w.r.	102.4	200.7	1.478	0.70670 ± 6	11.8
	plag, fresh	19.33	369.8	0.151	0.70543 ± 6	---
	plag, altered	30.15	423.1	0.206	0.70558 ± 8	---
	kspar	140.2	289.1	1.404	0.70642 ± 7	---
	biotite	332.3	22.46	42.85	0.74346 ± 23	---
S20a	w.r.	111.5	182.5	1.770	0.70696 ± 5	12.0
S7a	w.r.	113.7	173.0	1.902	0.70700 ± 4	11.8
S69a	w.r.	126.9	143.8	2.556	0.70747 ± 6	11.4
S7b	w.r.	110.6	93.0	3.444	0.70810 ± 8	13.2, 13.2, 13.3
Sedimentary Rocks						
Kodiak Formation						
M5c	argillite	83.9	105.5	2.304	0.71088 ± 6	---
U13a	graywacke	28.9	136.4	0.614	0.70738 ± 7	---
Shumagin Formation, Shumagin Islands						
N135a	argillite	125.3	190.0	1.910	0.70905 ± 6	14.9
N42b	argillite	93.9	171.4	1.586	0.70790 ± 5	13.5
N62	graywacke	54.0	246.0	0.635	0.70552 ± 4	12.9
NY90	graywacke	30.8	471.2	0.189	0.70471 ± 5	---
N16a	graywacke	31.44	405.8	0.224	0.70497 ± 7	13.4
N18b	graywacke	---	---	---	-----	12.8
N65	graywacke	---	---	---	-----	12.1
N233b	graywacke	---	---	---	-----	12.4
Shumagin Formation, Sanak Island						
S33e	argillite	97.2	164.9	1.706	0.70760 ± 7	14.8
S89d	argillite	85.9	181.5	1.370	0.70724 ± 4	14.6, 14.7

TABLE 3. (continued)

Sample	Rb ppm	Sr ppm	$^{87}Rb/^{86}Sr$	$^{87}Sr/^{86}Sr$ ± 2σ	$\delta^{18}O$ o/oo
S72d graywacke	24.5	407.2	0.175	0.70484 ± 5	11.6
S84f graywacke	33.76	492.3	0.199	0.70476 ± 6	13.2
Greenstone					
Ghost Rocks Formation, Kodiak Island 15-2e	7.0	142.0	---	-----	---

w.r. is whole rock.
Rb and Sr concentrations by isotope dilution for all samples except 15-2e (XRF).
Sr isotopes normalized to $^{86}Sr/^{88}Sr$ = 0.1194 and reported relative to Eimer & Amend SrCO3 = 0.70800.

[1973, 1976] for amphibolite melting, it is difficult to make firm estimates of melt compositions. In our models, we use D(Sr) = 1 and 2 to cover a range of likely residual mineral contents. Other authors concerned with modelling sediment melting have used similar figures [Arth and Hanson, 1975].

To consider the effects of melting amphibolite which may be intercalated with metasediments at depth in the prism, we use the Sr data from Hudson et al. [1979] for amphibolites in the Cretaceous Valdez Group near Prince William Sound (Figure 1), which may be in part correlative with the Kodiak and Shumagin formations. This parent is Amphibolite I in Table 4. Because the Sr contents of these amphibolites are quite low for basaltic rocks (58 ppm), we also consider a model amphibolite with a typical mid ocean ridge basalt (MORB) Sr content (135 ppm) (Amphibolite II in Table 4). D(Sr) will not be 1 for partial melting of amphibolite. Using Arth's basalt-andesite distribution coefficients and the residual phases reported by Helz [1976] for partial melting of Picture Gorge Basalt at 970°C, 5 kbar P_{H2O} (57% melt), we calculate D(Sr) = 0.24. Batch melts of amphibolite under these conditions will have Sr = 85 ppm (Amphibolite I) or 200 ppm (Amphibolite II). Basalt-related or -derived melts having more than or equal to 200 ppm Sr require negative sediment contributions for melting of metasedimentary rocks with D(Sr) = 1; thus we use Sr = 190 ppm for Amphibolite II in Table 4, which allows positive sediment contributions. No $\delta^{18}O$ data are available for the Alaskan amphibolites or greenstones. We have taken the mean $\delta^{18}O$ (+10.6 o/oo) of Franciscan Formation (California) metabasalts from Magaritz and Taylor [1976] for these amphibolite models, as examples of metabasalts within an accretionary prism.

Sources beneath the prism. Possible sources beneath the prism include ascending magmas from either the subducted slab (either MORB or remelted MORB) or the mantle wedge between the slab and the prism (arc magmas).

Ocean ridge basalt magma could be injected into the prism during subduction of an active ridge [Marshak and Karig, 1977] or perhaps by extrusion along a number of subducted, leaking transform faults. Alternatively, arc magma may have formed anomalously near the trench. Typical Sr and O data for MORB and arc magmas are given in Table 4. Remelted MORB would likely be in the amphibolite facies (ignoring the difficulties in melting basalt at shallow depth along the top of the subducted slab), and it would likely have suffered low-temperature alteration by exchange with seawater. Sr contents of altered seafloor basalts need not change, whereas both $^{87}Sr/^{86}Sr$ and $\delta^{18}O$ increase during low-temperature alteration [Hart, 1972; Hart et al., 1974; Muehlenbachs and Clayton, 1972; Spooner and Fyfe, 1973]. These effects have been taken into account in the Altered MORB end member in Table 4. The Sr content in the remelted, Altered MORB was determined as described above for the Amphibolite I and II models.

One additional effect must be noted. As they rise through the accretionary prism and begin to

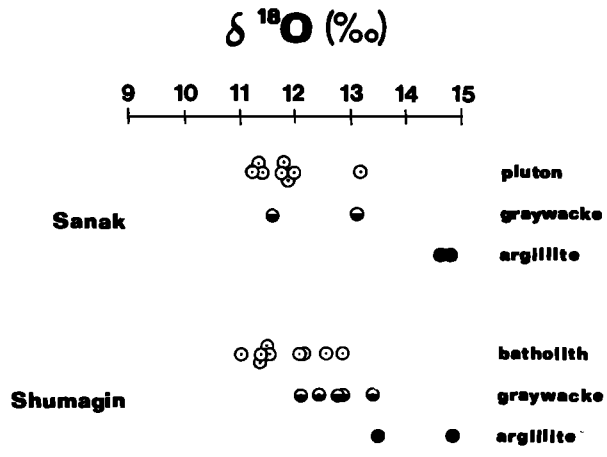

Fig. 5. Variations in $\delta^{18}O$ for intrusions and Shumagin Formation graywacke and argillite from the Sanak and Shumagin islands.

melt their wall rocks, these magmas must crystallize [Bowen, 1928; Taylor, 1978, 1980]; thus it is especially important to our models to estimate the change in Sr content as this occurs. We assume that D(Sr) = 1 for these magmas, which is not unreasonable. For example, Ewart et al. [1973] calculated that Tongan dacites were related to andesites by fractional crystallization of phenocryst assemblages which yield D(Sr) = 1.08 and 1.09 using Arth's [1976] distribution coefficients. Gill [1978] reached similar conclusions, noting the nearly constant Sr contents in several arc suites.

For other trace elements, the distribution coefficients will not be 1, so we must estimate the degree of fractionation required to produce a given amount of sediment melt. Taylor [1980] estimated that for hot wall rock, ratios of cumulates to assimilated wall rocks might approach 1:1, while for cool wall rock, ratios would exceed 3.25:1. We have no direct evidence on the thermal state of the accretionary prism 60 m.y. ago in the Kodiak-Shumagin-Sanak area. Hudson et al. [1979] described amphibolite-grade metamorphic rocks from the Chugach Mountains which correlate with the Kodiak and Shumagin formations. If that area represents a deeper section through the accretionary wedge, it is possible that the wall rocks to the intrusions may have been heated. This is not the normal case for subduction zones, but we are dealing with an anomalously situated igneous belt, which requires an unusual thermal regime.

Byrne [1979] suggested that the Kula-Farallon spreading ridge may have been quite close and parallel to the accretionary prism in the early Tertiary. If so, subduction of hot oceanic lithosphere may have generated unusually high temperatures in the overlying accretionary prism [DeLong et al., 1979]. We assume that the wall rocks were preheated to amphibolite grade, and that one part of basalt (by weight) must fractionate to form one part of sediment-derived melt.

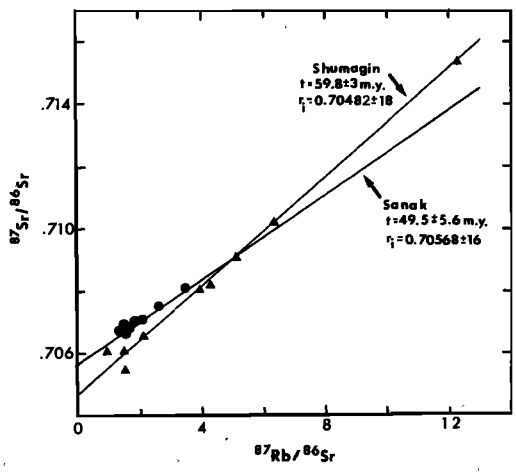

Fig. 6. Whole rock isochrons for the Shumagin batholith (triangles) and the Sanak pluton (circles) showing age and initial ratio. Reported uncertainties are 2σ of the mean. Analytical uncertainties of individual analyses are less than or equal to the size of the symbols.

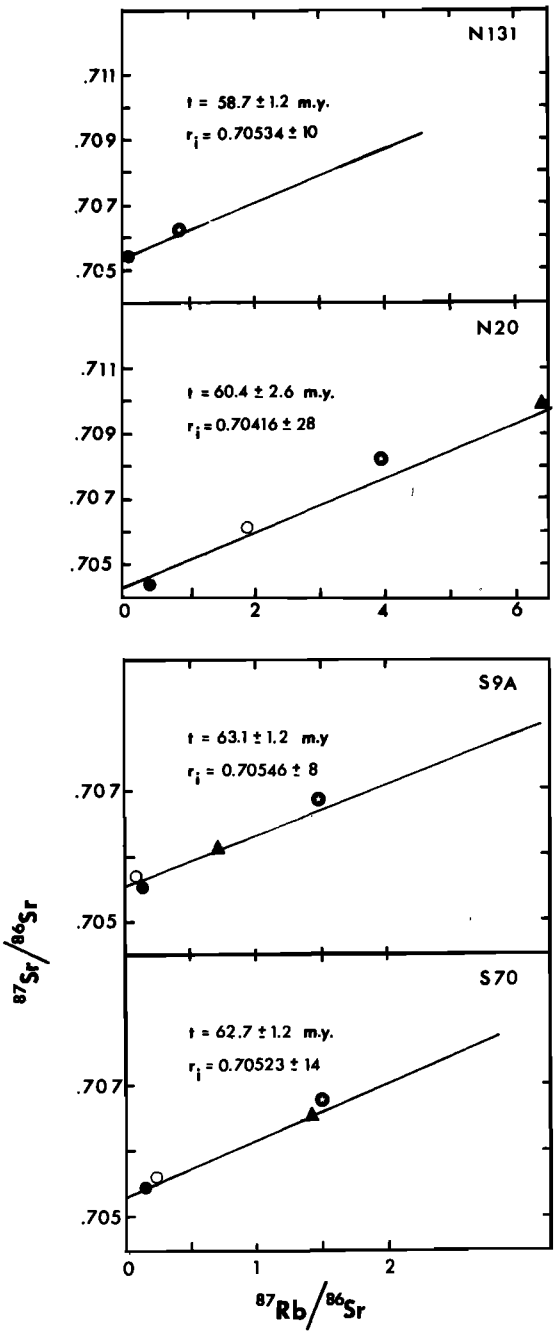

Fig. 7. Mineral isochrons for two samples from the Shumagin batholith (N131, N20) and two from the Sanak pluton (S9a, S70). Symbols used are fresh plagioclase (solid circles), altered plagioclase (open circles), K-feldspar (triangles), and whole rock (encircled stars). Isochrons are fitted using fresh minerals only, and all isochrons pass through biotite (not shown). Reported values are age and initial ratios; uncertainties are 2σ of the mean. Analytical uncertainties for individual analyses are less than or equal to the size of the symbol.

A last point to consider for the thermal effects, which may have a bearing on deciding between models involving 'primary' vs. remelted basalt, is the relative temperatures of MORB vs.

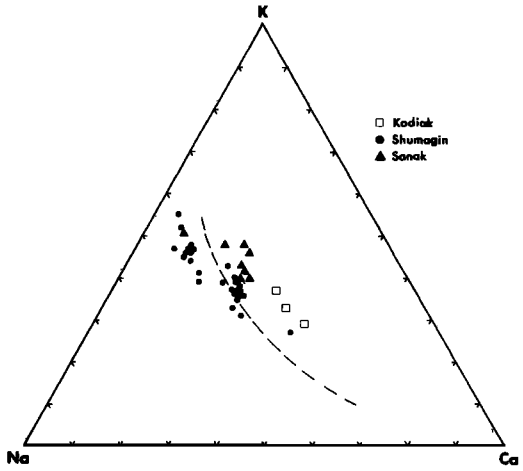

Fig. 8. Ca-Na-K diagram for Kodiak, Shumagin, and Sanak intrusions. Data are from Table 2 and Hill [1979]. Dashed line is average calc-alkaline trend, after Barker and Arth [1976].

remelted-MORB magmas. The liquidus temperature of ocean ridge tholeiite is approximately 1200°C [Tilley et al., 1972]. The temperatures of melts derived from water-saturated amphibolite would be much lower, up to 1000°C [Helz, 1976]. Therefore, a first-cycle basalt should be a more efficient melting agent within the prism than a second-cycle basalt, and would be more likely to be able to cause widespread melting to form batholiths.

We have used measured values where possible and typical analyses from the literature where necessary to characterize the Sr contents, $\delta^{18}O$, and $^{87}Sr/^{86}Sr$ of potential source materials which may have combined to form the intrusions exposed on the Kodiak, Shumagin and Sanak islands. These values, for graywacke, argillite, and amphibolite from within the prism, and for MORB, arc magma, and remelted-MORB from below the prism, are presented in Table 4a. In the following section we use these values and other trace element data to constrain the origin of the intrusions.

Origin of the Intrusions

Sr and O isotope constraints. In this section we will use the isotopic data to model the origin of the Sanak and Shumagin intrusions. Sr and O isotope correlations have been used by several workers to establish mixing models for igneous rocks [Magaritz et al., 1978; James, 1980; Taylor and Silver, 1978; Michard-Vitrac et al., 1980; Halliday et al., 1980; Taylor, 1980]. Theoretical calculations [Langmuir et al., 1978] indicate that samples related by simple mixing should form a smooth curvilinear array with, in the case of Sr vs. O, a positive correlation.

Data for the Shumagin batholith and the Sanak pluton are plotted on a $(^{87}Sr/^{86}Sr)_o$ vs. $\delta^{18}O$ diagram in Figure 9. The two intrusions define essentially horizontal arrays with limited variation in $\delta^{18}O$. The fact that the whole-rock samples are not positively correlated means that the samples do not represent mixing of different proportions of the same end members. Instead, the data are consistent with a model that generates each intrusion from a single batch melting or mixing process which yields a well mixed, homogeneous magma which is subsequently modified by fractional crystallization and alteration.

This is demonstrated again in Figure 10, where $(^{87}Sr/^{86}Sr)_o$ is plotted against (1/Sr). On this diagram, simple two-component end-member mixing is represented by a straight line. The effect of plagioclase fractionation is to shift samples horizontally to lower Sr contents, as indicated on the diagram. The purpose of this diagram is to illustrate that MORB, or melts derived from MORB or Amphibolite II can be mixed with melts derived from sediments of various graywacke: argillite ratios to produce melts with $^{87}Sr/^{86}Sr$ ratios and Sr contents typical of the least fractionated (lowest SiO2, highest Sr) Sanak and Shumagin intrusive samples. A similar set of lines could be drawn between the 'arc basalt magma' and the sediments if a different bulk D(Sr) were used for melting of the sediments.

In order to evaluate and quantify these models, we have carried out a series of calculations for the Sanak pluton. Compositions of possible end members, discussed in a previous section, are presented in Table 4a. The mixing proportions, listed in Table 4b, were determined by simultaneously solving two mass balance equations, one in terms of Sr contents and one for $^{87}Sr/^{86}Sr$ ratios equivalent to those of the least fractionated Sanak pluton sample. Thus, all combinations listed in Table 4b satisfy the constraints imposed by Sr contents and isotopic compositions (i.e., it is the numerical equivalent of Figure 10).

We tested all of these models by calculating the $\delta^{18}O$ that would result from mixing the end members in the proportions indicated. These values are listed in the column headed 'predicted $\delta^{18}O$' in Table 4b. Models are considered acceptable if they match the observed average $\delta^{18}O$ of the Sanak pluton (+11.6 o/oo) within ±10%. This allows a range in $\delta^{18}O$ of +10.4 to +12.8 o/oo.

Models 1, 2, and 3 in Table 4b refer to melting of sources within the accretionary prism. Model 1, melting of sediments only, clearly is unsatisfactory, because it yields $\delta^{18}O$ far higher than observed in the intrusions. Model 2, melting of sediments plus Amphibolite I, satisfies the oxygen constraints if a graywacke-rich sediment melts. Model 3, melting of sediments plus Amphibolite II, produces acceptable $\delta^{18}O$ for all sediment compositions tested.

The final test of any model is that it conform with geologic observations. In this case, we require that the end-member proportions be consistent with the observed geology of the accretionary prism. Both models 2 and 3 fail on this basis, because they require an accretionary wedge which is 50-92% amphibolite (making the simple assumption that amphibolite and metasediments would melt in proportion to their abundance in the prism - probably not true in reality).

We next consider models 4 through 6, which combine sediment melts with magmas derived from beneath the prism. Model 4, melting of sediments by an ascending, remelted MORB magma, matches the oxygen constraints if the sediments are argillite-rich. Model 5, melting of sediments by an ascending MORB-like magma, produces satisfactory

Table 4a. Sr Contents and Sr and O Isotopic Compositions of Possible End Members, With Sanak Pluton Data for Comparison

Component	Sr ppm	$^{87}Sr/^{86}Sr$	$\delta^{18}O$ o/oo
Sources within the prism			
Average graywacke, Sanak Is.	450.	0.70464	12.0
Average argillite, Sanak Is.	173.	0.70611	14.7
Amphibolite I[a]	58.5 (87. in melt)	0.7046	10.6
Amphibolite II	135. (190. in melt)	0.7046	10.6
Sources beneath the prism			
Altered MORB[b]	135. (190. in melt)	0.7039	8.8
MORB[c]	135.	0.7029	5.5
Arc basalt[d]	385.	0.7032	5.5
Sanak pluton	200.	0.70535	11.6

[a] Amphibolite I data from Hudson et al. [1979] and Magaritz and Taylor [1976].
[b] Altered MORB data from Spooner and Fyfe [1973] and Muehlenbachs and Clayton [1972].
[c] MORB data from Hart [1971], Hart and Brooks [1977], and Pineau et al. [1976].
[d] Arc basalt data from Kay [1977].

results for all but the 1:1 G:A mixture. Model 6, melting of sediments by an arc magma, was constructed using bulk D(Sr) = 2 for sediment melting (otherwise, the sediment melts have too much Sr to allow any match to be made). All models (1 through 6) were tested using both D(Sr) = 1 and 2. Models 1 through 5 (having a low-Sr mafic end member) require D(Sr) ≈ 1 for melting of the metasediments in order to satisfy the twin constraints of Sr contents and isotopic composition, while model 6 (having a high-Sr mafic end member) requires that D(Sr) ≈ 2 for metasediment melting.

Table 4b. Sr and O Model Calculations[a]

End Members	Mixing Proportions		Predicted $\delta^{18}O$
1. Sediments only	9.8% Graywacke	90.2% Argillite	14.5
2. Sediments plus Amphibolite I			
1:1 G:A[b]	50.3% Sediments	49.7% Amphibolite	12.1
1:3 G:A	72.9% Sediments	27.1% Amphibolite	13.2
1:5 G:A	85.7% Sediments	14.3% Amphibolite	13.8
3. Sediments plus Amphibolite II			
1:1 G:A	7.9% Sediments	92.1% Amphibolite	10.8
1:3 G:A	18.6% Sediments	81.4% Amphibolite	11.2
1:5 G:A	33.7% Sediments	66.3% Amphibolite	11.8
4. Sediments plus Altered MORB			
1:1 G:A	7.9% Sediments	92.1% MORB	9.2
1:3 G:A	18.6% Sediments	81.4% MORB	9.8
1:5 G:A	33.7% Sediments	66.3% MORB	10.7
5. Sediments plus MORB			
1:1 G:A	36.5% Sediments	63.5% MORB	8.4
1:3 G:A	60.3% Sediments	39.7% MORB	10.7
1:5 G:A	77.3% Sediments	22.7% MORB	12.3
6. Sediments plus Arc Basalt[c]			
1:3 G:A	86.1% Sediments	13.9% Basalt	12.8
1:5 G:A	80.1% Sediments	19.9% Basalt	12.5

[a] See text for details of models.
[b] G:A - graywacke:argillite ratio in the sedimentary component.
[c] Requires D(Sr) = 2 for melting of sedimentary component.

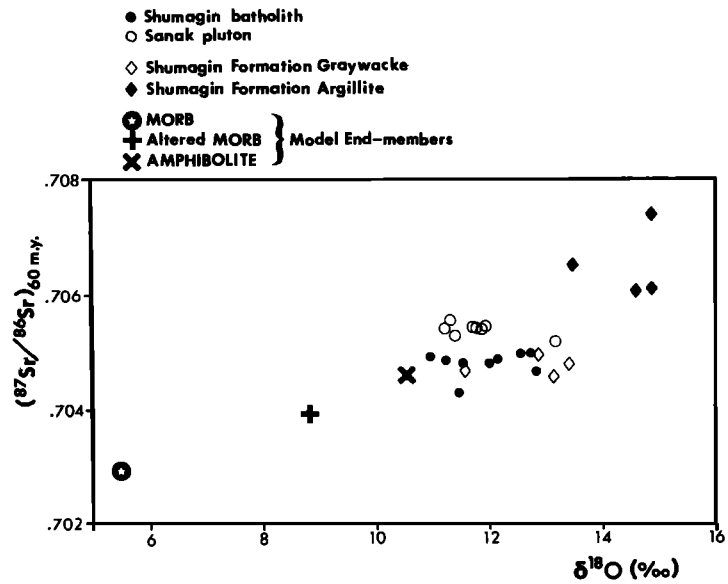

Fig. 9. $^{87}Sr/^{86}Sr$ (calculated for 60 m.y.) vs. $\delta^{18}O$ for the Sanak and Shumagin intrusions, Shumagin Formation sediments, and the end-member compositions chosen for melting models (taken from Table 4). See text for discussion.

Model 6 also provides a satisfactory match to the observed values of $\delta^{18}O$ in the intrusions.

Thus, all three models which involve a magma derived from beneath the prism are acceptable on the basis of the isotope modelling. None of them require a sediment composition which is inconsistent with the surface geology. In the context of the anomalous tectonic setting proposed for this region, all three mafic end members could be geologically reasonable. Therefore, all three models are considered acceptable at this stage, and will be tested against other trace elements in the following section.

Trace element constraints. In this section we examine the three preferred models from the preceding discussion using Rb, Sr, Ba, and the REE. In general, metasediment residues which contain major amounts of biotite, garnet, or hornblende are precluded because they retain too much Rb, Ba, and heavy rare earth elements (HREE). We focus on residues dominated by quartz and plagioclase, with minor garnet and trace

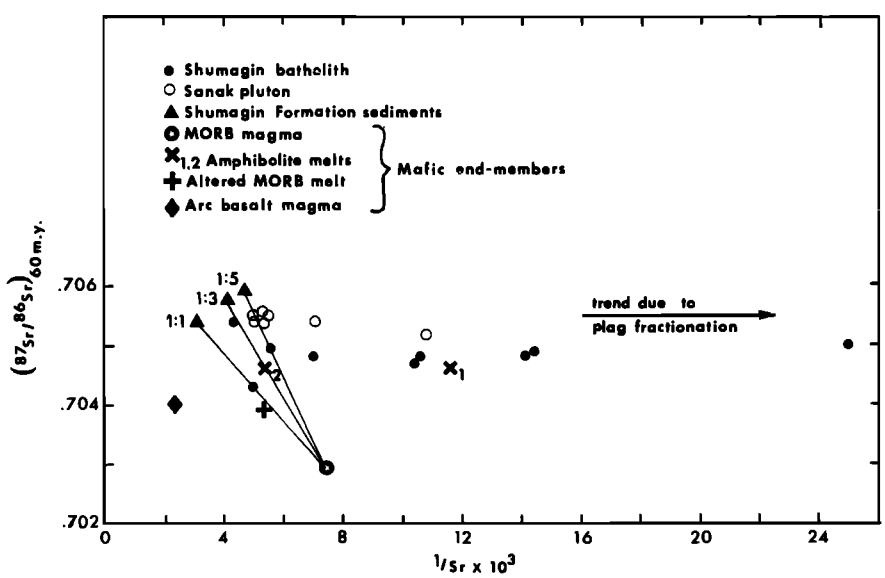

Fig. 10. Mixing diagram showing samples from the Sanak pluton, the Shumagin batholith, and various model end members. The Shumagin Formation sediments are labeled to indicate graywacke:argillite ratios. Values used for mafic end members are taken from Table 4. Straight lines are drawn from MORB to the three sediment mixtures to illustrate our model of MORB magma mixing with sediment melts to form a homogeneous mixture which is subsequently modified by plagioclase separation.

Table 5. Trace Element Compositions of Model Melts

	Starting Compositions				Model 4					Model 5			Model 6			Target Values	
	1	2	3	4	5	6	7	8	9	10	11	12	13	14	15	16	17
Rb	3.	10.	29.	92.	5.	11.	48.	150.	52.	7.	77.	104.	23.	110.	111.	97.	66.
Sr	135.	328.	450.	174.	180.	185.	450.[D(Sr)=1]	174.	197.	138.	193.	201.	305.	192.	186.	200.	231.
							321.[D(Sr)=2]	124.									
Ba	13.	115.	603.	908.	17.	38.	916.	1379.	464.	28.	771.	1013.	253.	1123.	1093.	898.	917.
La*	8.8x	29.1x	69.4x	68.5x	13.0x	29.4x	96.8x	95.6x	51.8x	20.0x	64.6x	78.6x	66.3x	91.8x	89.9x	75.5x	63.6x
Sm	14.4x	22.1x	19.7x	27.2x	17.0x	32.9x	24.4x	33.6x	32.6x	27.8x	28.2x	31.1x	46.4x	33.4x	34.9x	37.6x	29.5x
Eu	14.5x	18.8x	15.5x	18.4x	17.2x	29.0x	14.1x	16.8x	24.7x	24.6x	18.0x	18.2x	34.1x	18.6x	19.9x	18.7x	21.7x
Gd	13.4x	16.1x	16.2x	17.4x	15.0x	27.5x	16.8x	18.1x	24.3x	24.6x	19.0x	19.4x	32.8x	19.9x	20.9x	27.9x	21.0x
Yb	13.2x	13.5x	8.5x	11.0x	16.4x	30.0x	5.5x	7.0x	22.2x	24.1x	12.1x	10.7x	27.0x	9.5x	10.8x	12.1x	12.4x

Columns are described as follows.

1) MORB - sample 13-E, Kay et al. [1970]; Sr from Table 3 for continuity.
2) High alumina basalt, Taylor [1969].
3) Average graywacke, Sanak Island.
4) Average argillite, Sanak Island.
5) 63% melt of MORB using phase proportions from Helz [1976] and basalt D's from Arth [1976].
6) 60% crystallization of (5), using (0.5 plagioclase + 0.5 clinopyroxene); basalt D's from Arth [1976].
7) and 8) 60% melt of graywacke and argillite, respectively. Values shown for bulk D(Sr) = 1 and 2. Other trace elements calculated using rhyolite D's from Arth [1976] residue = (0.47 plagioclase + 0.47 quartz + 0.055 garnet + 0.005 apatite + 0.002 zircon). Apatite and zircon proportions after Hanson [1980].
9) Pluton predicted from model 4: (0.337 sediment melt from a 1:5 G:A source) + (0.663 fractionated, MORB remelt).
10) MORB from (1), 60 % crystallized using (0.5 plagioclase + 0.5 clinopyroxene), basalt D's from Arth [1976].
11) Pluton predicted from model 5: (0.603 sediment melt from a 1:3 G:A source) + (0.337 fractionated MORB).
12) Pluton predicted from model 5: (0.773 sediment melt from a 1:5 G:A source) + (0.227 fractionated MORB).
13) High alumina basalt from (2), 60% crystallized using (0.3 clinopyroxene + 0.06 orthopyroxene + 0.57 plagioclase + 0.07 oxide) after Ewart et al. [1973]; basalt D's from Arth [1976].
14) Pluton predicted from model 6: (0.861 sediment melt from a 1:3 G:A source) + (0.139 fractionated high alumina basalt).
15) Pluton predicted from model 6: (0.801 sediment melt from a 1:5 G:A source) + (0.199 fractionated high alumina basalt).
16) Least evolved sample, Sanak pluton (S8a).
17) Least evolved sample, Shumagin batholith (N131).

* Rare earths have been normalized to the chondrite average of Haskin et al. [1966].
Rb, Sr, and Ba data are in parts per million.

apatite and zircon. We have assumed 60% melting of the metasedimentary source, which requires 60% crystallization of the ascending mafic magmas, as discussed earlier. The results of our calculations are given in Table 5.

The ascending amphibolite melt (model 4) must be derived by at least 60% fusion; otherwise the melt will be so silicic that dacite amphibole D's are required, which yield very low HREE contents in the melt [Arth, 1976; Helz, 1976; Hanson, 1980]. An eclogite residue is not acceptable, again because the HREE in the melt would be too low. Fractionating either (plagioclase + clinopyroxene) or (plagioclase + hornblende) from this melt will yield generally similar trace element contents in fractionated liquids if basalt-andesite D's apply. This model does not give a satisfactory trace element match with the intrusions (compare column 9 with columns 16 and 17, Table 5), because of the large basalt component imposed by the higher $\delta^{18}O$ of the altered basalt parent.

Calculated trace elements for fractionated MORB mixing with melts derived from 1:3 and 1:5 G:A ratios are given in columns 11 and 12 of Table 5. This model yields a good overall match with the real intrusions (columns 16 and 17).

Finally, columns 14 and 15 of Table 4 show that a typical arc basalt (column 2, Table 4) can fractionate and mix with argillite-rich metasediment melts to form a generally satisfactory trace element match to the intrusions, although Ba and the LREE are somewhat high in the model plutons. Nevertheless, in view of the many estimates needed to construct the model, we feel that the results are close enough to make this a viable possibility for explaining the origin of the intrusions.

In summary, comparison of the Sr and O relationships in the intrusions vs. probable source materials rules out the possibility that the intrusions formed solely within the accretionary prism. Metasediments alone are not a suitable source. The high $\delta^{18}O$ of metabasalt in accretionary prisms forces a high proportion of this end member in the intrusions, which makes it impossible to match the abundances of other trace elements in the intrusions. Similar arguments rule out remelted MORB as a source. A magma with an isotopic and trace element content similar to MORB forms a close match in all respects. If the bulk $D(Sr) \approx 2$ during sediment melting, then an arc magma having typically higher Sr than MORB is a possible source, although it does not form as close a match for all trace elements. In the following section we briefly review possible reasons for this magmatic activity.

Tectonic Implications

It is probably not a coincidence that major episodes of both basaltic volcanism and intermediate plutonism occurred in or near the accretionary belt of southern and southwestern Alaska in early Tertiary time. The Paleocene Ghost Rocks Formation on Kodiak Island [G. W. Moore, 1969; Connelly, 1978; Hill, 1979; Reid and Gill, 1980] and the Paleocene and Eocene (?) Orca Group in Prince William Sound [Tysdal et al., 1977] contain abundant mafic to intermediate volcanic rocks intercalated with subaqueous clastic sediments ranging from conglomerate to graywacke and argillite. It is important to note that volcanism and coarse clastic sedimentation occurred simultaneously in these units, indicating that the source of the volcanism was active quite near the continental margin and, by inference, the subduction zone.

The cause of the volcanism remains uncertain, if indeed a single mechanism can explain all of it. Most of the rocks have been metamorphosed, which makes it difficult to interpret their source. Tysdal et al. [1977] suggested that the Orca Group represents volcanism along a leaky transform fault. Reid and Gill [1980] described two groups of volcanics within the Ghost Rocks Formation, one tholeiitic and one calc-alkaline. Sample 15-2e (Table 1) is from the latter group, and calculations (not shown) suggest that this sample has suitable trace element concentrations to act as the mafic component in the granitic intrusions. We feel that the origin of the intrusions will not be completely understood until the origin of the Ghost Rocks Formations volcanism is explained, a study of which is in progress (M. Reid, manuscript in preparation, 1981).

Although Marshak and Karig [1977] suggested that the early Tertiary intrusions within the accretionary prism formed when the Kula-Farallon ridge was subducted at a high angle to the trench, Byrne [1979] reinterpreted the magnetic anomalies in the northeast Pacific to suggest that the ridge was adjacent and subparallel to the continental margin of southwestern Alaska. Whether or not the Kula-Farallon ridge was actually subducted as an active ridge, we believe that the volcanics of the Ghost Rocks Formation and the Orca Group are probably related to Kula-Farallon ridge activity and that the Kodiak, Shumagin, and Sanak intrusions represent hybrids formed when similar magma from the same source intruded the prism.

The Ghost Rocks Formation is intruded by satellites of the Kodiak batholith [Hudson et al., 1979; Hill, 1979], and thus it predates the intrusion. The short time period between emplacement of the Ghost Rocks Formation and intrusion of the Kodiak batholith, discussed earlier, is sufficiently short to allow a genetic relationship, perhaps not by the same pulse which formed the Ghost Rocks Formation flows but of similar material produced at most 3 to 5 m.y. later.

Some such anomalous source is required to explain the early Tertiary magmatism in the accretionary prism because 'normal' (?) arc magmatism, which was centered on and north of the Alaska Peninsula throughout the active periods of the Mesozoic and Cenozoic, occurred there simultaneously with the activity in the accretionary belt [Hudson 1979]. The Paleocene to Eocene Tolstoi Formation on the Alaska Peninsula contains abundant volcanic flows and detritus [Burk, 1965], suggesting that volcanism was coincident with this accretionary pulse. A temporary outward shift of the subduction zone to explain the magmatism within the accretionary belt, proposed by Kienle and Turner [1976] and G. W. Moore [1980], does not explain the continuity of 'normal' arc activity in its accustomed place during the time the 'anomalous' igneous rocks were being emplaced in the accretionary terrane.

Any models which attempt to reconcile the geology of southwestern Alaska in the early Tertiary with the position of ridges, etc., in the northeastern Pacific encounter a major problem, in that the exact location or orientation of southwestern Alaska 60 m.y. ago is not known. Much of Alaska south of the Denali fault consists of a number of allocthonous blocks, which formed somewhere to the south before being emplaced against northern Alaska [Jones et al., 1977; Hillhouse, 1977; Packer and Stone, 1974; Packer et al., 1975; Stone and Packer, 1977]. The work of Packer, Stone, and coworkers suggests that southwestern Alaska has had a complex history beginning far to the south of its present location, finally being emplaced against northern Alaska perhaps in post-Eocene time. While it seems clear that the Kodiak-Shumagin-Sanak accretionary terrane and the Alaska Peninsula arc terrane were part of the same block 60 m.y. ago, we must await more detailed paleomagnetic studies of Paleocene and Eocene rocks from this region before we can be sure how to relate the nature and timing of events within the arc and accretionary terranes with inferred positions of seafloor features.

Implications for I- vs. S-Type Granitoids

Chappell and White [1974] and O'Neil et al. [1977] listed criteria to distinguish between granitic rocks formed by melting igneous materials (I-type) and those formed by melting sedimentary materials (S-type) in eastern Australia. The intrusions we report possess both S-type and I-type characteristics. Among the S-type traits are the lack of hornblende and sphene, the presence of sedimentary-derived xenoliths which contain aluminosilicates and garnet, and $\delta^{18}O$ values > +10.0 o/oo. Among the I-type traits are the rarity of primary muscovite, linear variation diagrams for some elements, relatively high Na2O contents, and $^{87}Sr/^{86}Sr < 0.706$. Not all samples have >1% normative corundum, as in the S-type definition. This ambiguity results from the hybrid nature of the intrusions, in that both I-type ('basalt') and S-type material is present. To add to the complexity, much of the Upper Cretaceous Kodiak and Shumagin formations is composed of young volcanogenic detritus; thus, the S component itself has a significant I component. These complexities suggest that, although the I vs. S concept may be a useful one, blind application of the limits defined in one area may lead to spurious conclusions in another.

Summary

The 60 m.y. intrusions on the Kodiak, Shumagin, and Sanak islands represent an anomalous magmatic event which occurred over 100 km nearer the trench than the contemporaneous main locus of arc activity, centered on and north of the Alaska Peninsula. The metamorhpic xenocrysts and xenoliths suggest the presence of a crustal component within the intrusions. The strontium and oxygen isotope compositions and strontium contents require that an additional component, having lower $^{87}Sr/^{86}Sr$ and $\delta^{18}O$, be present as well if the crustal component was similar to the presently exposed Upper Cretaceous sedimentary rocks of the accretionary prism. Basalt is an obvious choice for this component, either as first-cycle magma generated from the mantle or as second-cycle, remelted basalt derived from the subducted slab. Partial melting models using proportions of end members deduced from the Sr and O relations suggest that first-cycle basalt better explains the trace element patterns observed in the intrusions. MORB is a suitable parent, as is the Paleocene Ghost Rocks Formation sample 15-2e. Typical arc basalts having Sr > 200 ppm may be suitable if the bulk D for Sr during metasediment melting was approximately 2. The mafic volcanics of the Ghost Rocks Formation and the Kodiak-Shumagin-Sanak intrusions may be genetically related, both ultimately derived from the Kula-Farallon ridge activity. This ridge may have been adjacent to or subducted beneath the accretionary prism 60 m.y. ago.

Acknowledgments. Part of this work was submitted by Hill in partial fulfillment of Ph.D. requirements at the University of California at Santa Cruz, and part was undertaken during Hill's tenure as National Research Council Postdoctoral Fellow with the U.S. Geological Survey. Work in Alaska and at Santa Cruz was supported by NSF grant EAR74-13266A01, ACS grant PRF-2884-G3, and grants from Exxon, Union Oil Company, the Chancellor's Patent Fund of the University of California, and the Penrose Bequest Fund of the Geological Society of America. The Alaska Branch of the U.S. Geological Survey provided logistical support in the field. The Sr isotopic data were acquired in Stan Hart's lab, supported by NSF grant 7803342-EAR. Casey Moore kindly provided the Sanak and Shumagin samples analyzed in this study. Jim Gill's expertise in setting up the Santa Cruz XRF lab and in supervising Hill's thesis are appreciateed. Fred Frey, L.A. Haskin, and Hugh Millard provided access to their neutron activation labs, and Doug Blanchard, Joyce Brannon, Jeff Jacobs, and Roy Knight made room in their busy schedules to help get the data out. We are grateful to each of these people and institutions for their support. Discussions with or critical reviews by Fred Barker, G. C. Brown, Tim Byrne, Fred Frey, Jim Gill, Stan Hart, Travis Hudson, Bob Kay, Casey Moore, Zell Peterman, Mary Reid, and Nobu Shimizu have helped focus our thinking on these rocks.

References

Arth, J. G., Behavior of trace elements during magmatic processes - A summary of theoretical models and their applications, J. Res. U.S. Geol. Surv., 4, 41-47, 1976.

Arth, J. G., and G. N. Hanson, Geochemistry and origin of the early Precambrian crust of northeastern Minnesota, Geochim. Cosmochim. Acta, 39, 325-362, 1975.

Barker, F., and J. G. Arth, Generation of trondhjemite-basalt suites, Geology, 4, 596-600, 1976.

Bateman, P. C., L. D. Clark, N. K. Huber, J. G. Moore, and C. D. Rinehart, The Sierra Nevada batholith: A synthesis of recent work across the central part, U.S. Geol. Surv. Prof. Pap., 414-D, 46 pp., 1963.

Beikman, H., Preliminary geologic map of Alaska,

U.S. Geol. Surv., Reston, Va., 1978.
Berg, E., Crustal structure in Alaska, Tectonophysics, 20, 165-182, 1973.
Bowen, N. L., The Evolution of the Igneous Rocks, Princeton University Press, Princeton, N. J., 1928.
Burk, C. A., Geology of the Alaska Peninsula - Island arc and continental margin, parts 1, 2, 3, Mem. Geol. Soc. Am., 99, 1965.
Byrne, T., Late Paleocene demise of the Kula-Pacific spreading center, Geology, 7, 341-344, 1979.
Chappell, B. W., and A. J. R. White, Two contrasting granite types, Pac. Geol., 8, 173-174, 1974.
Clayton, R. N., and T. K. Mayeda, The use of bromine pentafluoride in the extraction of oxygen from oxides and silicates for isotopic analysis, Geochim. Cosmochim. Acta, 27, 43-52, 1963.
Connelly, W., Uyak Complex, Kodiak Islands, Alaska: A Cretaceous subduction complex, Geol. Soc. Am. Bull., 89, 755-769, 1978.
Connelly, W., and J. C. Moore, Geologic map of the northwestern side of the Kodiak Islands, Alaska, U.S. Geol. Surv. Open File Map, 77-382, 1977.
Creasy, J. W., G. N. Eby, and S. A. Wood, Geochemistry of the Hart Ledge Complex, White Mountain batholith, New Hampshire, Geol. Soc. Am. Abstr. Programs, 11, 406, 1979.
Crecraft, H. R., W. P. Walsh, and S. H. Evans, Jr., Chemical evolution and development of compositional gradients in a silicic magma, Geol. Soc. Am. Abstr. Programs, 11, 406, 1979.
DeLong, S., W. Schwarz, and R. Anderson, Thermal effects of ridge subduction, Earth Planet. Sci. Lett., 44, 239-246, 1979.
Dostal, J. and S. Capedri, Uranium in metamorphic rocks, Contrib. Mineral. Petrol., 66, 409-414, 1978.
Ewart, A., W. B. Bryan, and J. B. Gill, Mineralogy and geochemistry of the younger volcanic islands of Tonga, S.W. Pacific, J. Petrol., 14, 429-465, 1973.
Faure, G., Principles of Isotope Geology, John Wiley and Sons, New York, 1977.
Fisher, M. A., and M. L. Holmes, Large-scale structure of deep strata beneath Kodiak shelf, Alaska, Geol. Soc. Am. Bull., 91, 218-224, 1980.
Frey, F. A., and B. W. Chappell, Granites from southeast Australia: Constraints on source mineralogy and composition imposed by rare earth element abundances, Geol. Soc. Am. Abstr. Programs, 11, 428, 1979.
Friedman, I., and J. D. Gleason, A new silicate intercomparison standard for ^{18}O analysis, Earth Planet. Sci. Lett., 18, 124, 1973.
Gill, J. B., Role of trace element partition coefficients in models of andesite genesis, Geochim. Cosmochim. Acta, 42, 709-724, 1978.
Grantz, A., Aerial reconnaissance of the outer Shumagin Islands, Alaska, U.S. Geol. Surv. Prof. Pap., 475-B, B106-B109, 1963.
Halliday, A. N., W. E. Stephens, and R. S. Harmon, Rb-Sr and O isotopic relationships in three zoned Caledonian granitic plutons, Southern Uplands, Scotland: Evidence for varied sources and hybridisation of magmas, J. Geol. Soc. London, 137, 329-348, 1980.
Hanson, G. N., Rare earth elements in petrogenetic studies of igneous systems, Annu. Rev. Earth Planet. Sci., 8, 371-406, 1980.
Hardenbol, J., and W. A. Berggren, A new Paleogene numerical time scale, in Contributions to the Geologic Time Scale, AAPG Stud. in Geol. #6, pp. 213-234, Am. Assoc. Pet. Geol., Tulsa, 1978.
Hart, S. R., K, Rb, Cs, Sr and Ba contents and Sr isotope ratios of ocean floor basalts, Philos. Trans. R. Soc. London, Ser. A, 268, 573-587, 1971.
Hart, S. R., and C. Brooks, The geochemistry and evolution of the early Precambrian mantle, Contrib. Mineral. Petrol., 61, 109-128, 1977.
Hart, S. R., A. J. Erlank, and E. J. D. Kable, Seafloor basalt alteration: Some chemical and Sr isotopic effects, Contrib. Mineral. Petrol., 44, 219-230, 1974.
Harvey, P. K., D. M. Taylor, R. D. Hendry and K. Bancroft, An accurate fusion method for the analysis of rocks and chemically related materials by X ray fluorescence spectrometry, X-Ray Spectrom., 2, 33-44, 1973.
Haskin, L. A., F. A. Frey, R. A. Schmitt, and R. H. Smith, Meteoritic, solar and terrestrial rare-earth distributions, in Physics and Chemistry of the Earth, vol. 7, edited by L. H. Ahrens et al., pp. 167-321, Pergammon, New York, 1966.
Helz, R. T., Phase relations of basalts in their melting range at PH2O = 5 kb. as a function of oxygen fugacity, J. Petrol., 14, 249-302, 1973.
Helz, R. T., Phase relations of basalts in their melting range at PH2O = 5 kb., part II, Melt compositions, J. Petrol., 17, 139-193, 1976.
Hill, M. D., Volcanic and plutonic rocks of the Kodiak-Shumagin Shelf, Alaska: Subduction deposits and near-trench magmatism, Ph. D. thesis, Univ. of Calif., Santa Cruz, 1979.
Hillhouse, J. W., Paleomagnetism of the Triassic Nikolai Greenstone, McCarthy Quadrangle, Alaska, Can. J. Earth. Sci., 14, 2578-2592, 1977.
Hudson, T., Mesozoic plutonic belts in Southern Alaska, Geology, 7, 230-234, 1979.
Hudson, T., G. Plafker, and Z. E. Peterman, Paleogene anatexis along the Gulf of Alaska margin, Geology, 7, 573-577, 1979.
Jacobs, J. W., R. L. Korotev, D. P. Blanchard, and L. A. Haskin, A well-tested procedure for instrumental neutron activation analysis of silicate rocks and minerals, J. Radioanal. Chem., 40, 93-114, 1977.
James, D. E., Oxygen and strontium isotopic composition of Quaternary andesites from the Andes of S.W. Colombia, Year Book Carnegie Inst. Washington, 79, 452-455, 1980.
Jones, D. L., N. L. Silberling, and J. Hillhouse, Wrangellia - A displaced terrane in northwestern North America, Can. J. Earth Sci., 14, 2565-2577, 1977.
Karig, D. E., and G. F. Sharman, Subduction and accretion in trenches, Geol. Soc. Am. Bull., 86, 377-389, 1975.
Kay, R. W., Geochemical constraints on the origin of Aleutian magmas, in Island Arcs, Deep Sea Trenches and Back-Arc Basins, pp. 229-242, edited by M. Talwani and W. C. Pitman, AGU, Washington, D. C., 1977.
Kay, R. W., N. J. Hubbard, and P. W. Gast,

Chemical characteristics and origin of oceanic ridge volcanic rocks, J. Geophys. Res., 75, 1585-1610, 1970.
Kienle, J., and D. L. Turner, The Shumagin-Kodiak batholith - A Paleocene magmatic arc?, Geol. Rep. 51, pp. 9-11, Alaska Dep. of Nat. Res., Juneau, 1976.
Langmuir, C. H., R. D. Vocke, G. N. Hanson, and S. R. Hart, A general mixing equation with applications to Icelandic basalts, Earth Plan. Sci. Lett., 37, 380-392, 1978.
Lanphere, M. A., and D. L. Jones, Cretaceous time scale from North America, in Contributions to the Geologic Time Scale, AAPG Stud. in Geol. #6, pp. 259-268, Am. Assoc. Pet. Geol., Tulsa, 1978.
Luddington, S., W. N. Sharp, D. McKowan, and F. Barker, The Redskin granite - A Proterozoic example of thermogravitational diffusion?, Geol. Soc. Am. Abstr. Programs, 11, 469, 1979.
Luth, W. C., R. H. Jahns, and O. F. Tuttle, The granite system at pressures 4 to 10 kilobars, J. Geophys. Res., 69, 759-773, 1964.
Magaritz, M., and H. P. Taylor, Jr., Oxygen, hydrogen and carbon isotope studies on the Franciscan Formation, Coast Ranges, California, Geochim. Cosmochim. Acta, 40, 215-234, 1976.
Marshak, R. S., and D. E. Karig, Triple junctions as a cause for anomalously near-trench igneous activity between the trench and volcanic arc, Geology, 5, 233-236, 1977.
Matsuhisa, Y., O. Matsubaya, and H. Sakai, Oxygen isotope variations in magmatic differentiation processes of the volcanic rocks in Japan, Contrib. Mineral. Petrol., 39, 277-288, 1973.
Michard-Vitrac, A., F. Albarede, C. Dupuis, and H. P. Taylor, Jr., The genesis of Variscan (Hercynian) plutonic rocks: Inferences from Sr, Pb, and O studies on the Maldeta Complex, Central Pyrenees, Contrib. Mineral. Petrol., 72, 57-72, 1980.
Miller, C. F., and D. W. Mittlefehldt, Rare earth element depletion accompanying differentiation of felsic plutonic rocks, Geol. Soc. Am. Abstr. Programs, 11, 479-480, 1979.
Moore, G. W., Preliminary geologic map of Kodiak Island and vicinity, U.S. Geol. Surv. Open File Rep., 271, 1967.
Moore, G. W., New formations of Kodiak and adjacent islands, Alaska, U.S. Geol. Surv. Bull., 1274-A, A27-A35, 1969.
Moore, G. W., Arc-type volcanic rocks anomalously near oceanic trenches, Geol. Soc. Am. Abstr. Programs, 12, 142-143, 1980.
Moore, J. C., Complex deformation of Cretaceous trench deposits, southwestern Alaska, Geol. Soc. Am. Bull., 84, 2005-2020, 1973a.
Moore, J. C., Cretaceous continental margin sedimentation, southwest Alaska, Geol. Soc. Am. Bull., 84, 595-614, 1973b.
Moore, J. C., Geologic and structural map of the outer Shumagin Islands, southwestern Alaska, U.S. Geol. Surv. Misc. Invest. Ser. Map, I-815, 1974a.
Moore, J. C., Geologic and structural map of the Sanak Islands, southwestern Alaska, U.S. Geol. Surv. Misc. Invest. Ser. Map, I-817, 1974b.
Muehlenbachs, K., and R. N. Clayton, Oxygen isotope studies of fresh and weathered submarine basalts, Can. J. Earth Sci., 9, 172-184, 1972.
Nilsen, T. H., and G. W. Moore, Reconnaissance study of Upper Cretaceous to Miocene stratigraphic units and sedimentary facies, Kodiak and adjacent islands, Alaska, U.S. Geol. Surv. Prof. Pap., 1093, 34, 1979.
Norrish, K., and J. T. Hutton, An accurate X-ray spectrographic method for the analysis of a wide range of geological samples, Geochim. Cosmochim. Acta, 33, 431-453, 1969.
O'Neil, J. R., S. E. Shaw, and R. H. Flood, Oxygen and hydrogen isotope compositions as indicators of granite petrogenesis in the New England batholith, Australia, Contrib. Mineral. Petrol., 62, 313-328, 1977.
Packer, D. R., and D. B. Stone, Paleomagnetism of Jurassic rocks from southern Alaska, and their tectonic implications, Can. J. Earth Sci., 11, 979-997, 1974.
Packer, D. R., G. E. Brogan, and C. B. Stone, New data on plate tectonics of Alaska, Tectonophysics, 29, 84-102, 1975.
Peacock, M. A., Classification of igneous rocks, J. Geol., 39, 65-67, 1937.
Pineau, F., M. Javoy, J. W. Hawkins, and H. Craig, Oxygen isotope variations in marginal basin and ocean-ridge basalts, Earth Planet. Sci. Lett., 28, 299-307, 1976.
Reed, B. L., and M. A. Lanphere, Age and chemistry of Mesozoic and Tertiary plutonic rocks in south-central Alaska, Geol. Soc. Am. Bull., 80, 23-44, 1969.
Reed, B. L., and M. A. Lanphere, Alaska-Aleutian Range batholith - geochronology, chemistry and relation to circum-Pacific plutonism, Geol. Soc. Am. Bull., 84, 2583-2610, 1973.
Reid, M., and J. B. Gill, Near-trench volcanism, Kodiak Island, Alaska: Implications for ridge-trench encounter, Geol. Soc. Am. Abstr. Programs, 12, 148-149, 1980.
Savin, S. M., and S. Epstein, The oxygen and hydrogen isotope geochemistry of clay minerals, Geochim. Cosmochim. Acta, 34, 25-42, 1970.
Shaw, D. M., Geochemistry of pelitic rocks, part III, Major elements and general geochemistry, Geol. Soc. Am. Bull., 67, 25-42, 1956.
Shor, G. G., Jr., Seismic refraction studies off the coast of Alaska: 1956-1957, Bull. Seismol. Soc. Am., 52, 37-57, 1962.
Sighinolfi, G. P., and C. Gorgoni, Chemical evolution of high-grade metamorphic rocks - Anatexis and remotion of material from granulite terrains, Chem. Geol., 22, 157-176, 1978.
Spooner, E. T. C., and W. S. Fyfe, Sub-sea-floor metamorhpism, heat and mass transfer, Contrib. Mineral. Petrol., 42, 287-304, 1973.
Steiger, R. H., and E. Jaeger, Subcomission on geochronology: Convention on the use of decay constants in geo- and cosmo-chemistry, Earth Planet. Sci. Lett., 36, 359-362, 1977.
Stone, D. B., and D. R. Packer, Tectonic implications of Alaska Peninsula paleomagnetic data, Tectonophysics, 37, 183-201, 1977.
Streckeisen, A. L., Plutonic rocks - Calssification and nomenclature recommended by the IUGS subcommission on the systematics of igneous rocks, Geotimes, 18(10), 26-30, 1973.
Taylor, H. P., Jr., Oxygen and hydrogen isotope studies of plutonic granitic rocks, Earth Planet. Sci. Lett., 38, 177-210, 1978.
Taylor, H. P., Jr., and L. T. Silver, Oxygen isotope relationships in plutonic igneous rocks

of the Peninsular Ranges batholith, Southern and Baja California, U.S. Geol. Surv. Open-File Rep., 78-701, 423-426, 1978.

Taylor, S. R., Trace element chemistry of andesites and associated calcalkaline rocks, Proceedings of the Andesite Conference, edited by A. R. McBirney, State of Oregon, Dep. Geol. Miner. Res. Bull., 65, pp. 43-64, 1969.

Tilley, C. E., R. N. Thompson, and P. A. Lovenbury, Melting relations of some oceanic basalts, Geol. J., 8, 59-64, 1972.

Turner, D. L., R. B. Forbes, and C. W. Naeser, Radiometric ages of Kodiak Seamount and Giacomini Guyot, Gulf of Alaska - Implications for circum-Pacific tectonics, Science, 182, 579-581, 1973.

Tuttle, O. F., and N. L. Bowen, Origin of granite in the light of experimental studies in the system $NaAlSi_3O_8$-$KAlSi_3O_8$-SiO_2-H_2O, Geol. Soc. Am. Mem., 74, 1958.

Tysdal, R. G., J. E. Case, G. R. Winkler, and S. H. B. Clark, Sheeted dikes, gabbro and pillow basalt in flysch of coastal southern Alaska, Geology, 5, 377-383, 1977.

White, A. J. R., and B. W. Chappell, Ultrametamorphism and granitoid genesis, Tectonophysics, 43, 7-22, 1977.

(Received October 31, 1980;
revised May 4, 1981;
accepted May 19, 1981.)